

About CMBR

Gerd Pommerenke

Email: gerdpommerenke@arcor.de

Abstract

Because the CMBR follows the PLANCK's radiation law more or less exactly, it should, because of the indistinguishability of individual photons, apply to a whatever black emitter. Therefrom arises the guess, that the existence of an upper cut-off frequency of the vacuum could be the cause for the decrease in the upper frequency range. Since the lower-frequent share of the curve correlates with the frequency response of an oscillating circuit with the Q-factor $\frac{1}{2}$, it is examined, whether it succeeds to approximate the Planck curve by multiplication of the initial curve with the dynamic, time-dependent frequency response of the above mentioned model. Reason of the time-dependence is the expansion of the universe.

This work is based on a model published in [7]. It is shown, that the PLANCK graph can be approximated by application of the cumulative frequency response given by the model, upon the spectrum of an oscillatory circuit with the Q-factor $\frac{1}{2}$. Furthermore the progression of frequency, energy and entropy is analyzed. The results point out, that origin and progression of the CMBR have elapsed in a totally different manner than generally assumed. Because photons behaved like neutrinos immediately after BB they did not interact with other matter then. Thus, we can exactly calculate back to $8.42 \cdot 10^{-67}$ s instead of 379,000 years after BB.

Keywords: Cosmology, Big Bang Cosmology, Physics, Astronomy, Radio Astronomy, Wave Propagation, Expansion, Statistics, Thermodynamics, Relativistic Thermodynamics, Thermal Radiation, CMBR, Red-shift, Hubble-Parameter, Metrology.

1st edition Augsburg 2023

Contents

1.	Fundamentals	2
2.	Frequency relations	2
3.	The WIEN displacement law and the source-function.....	6
4.	Solution and analysis	10
5.	The WIEN displacement	18
6.	The temperature of the CMBR.....	20
7.	Energy and entropy of the CMBR	22
8.	Summary	33
9.	Affidavit.....	33
10.	Notes on the Appendix.....	33
11.	References.....	36

1. Fundamentals

This article is based on a model I published in [1] and later in [7]. The idea stems from Prof. Cornelius LANZOS, outlined in a lecture on the occasion of the EINSTEIN-symposium 1965 in Berlin. The lecture is put in front the work in [1]. It defines the expansion of the universe as a consequence of the existence of a metric wave-field. The temporal function of that field is based on the hypergeometric function ${}_0F_1 = J_0\sqrt{2\kappa_0 t/\varepsilon_0}$, used in form of the Hankel-function. The particular qualities of the function lead to an increase of the wavelength. In this connection the phase angle $2\omega_0 t = Q_0$ plays an important role, being identical with the frame of reference, affecting all proportions within the system. The value ω_0 corresponds to the PLANCK frequency. With the metric wave-field it's about an EM four-legged-field including vortices shaped as HERTZian dipoles arranged in form of a (regular) face-centered cubic (fc) crystal with the lattice-constant of the PLANCK-length. I named the vortices Metric Line Elements (MLE) and they are genuine physical objects.

This version considers the correction of a calculating error in [1], effecting the frequency- and phase-response as well as the phase- and group delay. Furthermore, an updated value of H_0 is used, based on the electron mass specified in [6]. In the annex the new Concerted International System of Units from [6] is used, but it doesn't have any effect to the result except for, that the calculation error is minimized. The model works with variable natural »constants«. But most of the resulting variations cancel each other. Only the LORENTZ-share remains. Thus, it's about a *Virtual Relativity Principle*.

A special solution of the MAXWELL equations was found for the Hankel-function with overlaid interference function, which describes the wave-propagation in the vacuum and co-cludes the expansion. This special solution owns an inherent propagation-velocity in reference to the empty space (subspace) which is almost zero to the current point of time.

One conclusion from the model is the existence of an upper cut-off frequency of the vacuum, which could not be detected until now, because its value is about magnitudes greater than the technically feasible one. Another conclusion of the model is the supposition that each photon is connected really or/and virtually with an origin at $Q_0 = 1/2$. That is the frequency, at which the excessive energy with the shape of the metric wave-function has been coupled into the very same one, as an overlaid wave, where it can be observed until now as cosmic microwave background-radiation (CMBR). Furthermore could be determined, that the bandwidth in the lower frequency range exactly matches the one of an oscillatory circuit with the Q-factor $1/2$, which equals the conditions to the point of time of the input coupling. An exceptional feature of the model is, that the Q-factor of the oscillatory circuit increases continuously equalling the above mentioned phase angle $2\omega_0 t = Q_0$ exactly.

Hence the intention of this article is, to determine, whether the PLANCK's graph can be approximated by application of the frequency response given by the model, upon the spectrum of an oscillatory circuit with the Q-factor $1/2$, furthermore to compare the calculated radiation temperature with the measured one.

2. Frequency relations

Since the cosmic background-radiation exactly follows the PLANCK's radiation law more or less, it should, because of the indistinguishability of individual photons, apply to a whatever black emitter. Therefrom arises the guess, that the existence of an upper cut-off frequency of the vacuum could be the cause for the weird curve regression in the upper frequency range.

Another aim of this article is, to improve the proceeding any farther in order to make more precise statements. With the model attention should be paid to the fact, that with some many exceptions (c, μ_0 , ε_0 , κ_0 , k), most of the fundamental physical constants are time- and refe-

rence-frame-dependent. They are marked with a tilde (\sim) being simple values while the actual variables are written without. And there is a conductivity of subspace κ_0 different from zero. The model is based on the PLANCK units, which can be determined by the locally measurable values (e.g. ω_0). On the one hand, it suggests the values of the universe as a whole (e.g. H_0), on the other hand, the values of the so called subspace (e.g. $\epsilon_0 = \text{const}$). That's the medium the metric wave field is propagating in. The proportionality factor is the phase angle of the temporal function $Q_0 = 2\omega_0 t$.

The model is based on the fact, that electromagnetic waves don't propagate independently, but as interferences (overlaid) of the metric wave field. The wave length of the metric wave field is equal to the PLANCK-length and proportional Q . In return, the wave length of overlaid waves is proportional $Q^{3/2}$. To the frequencies $\omega_0 \sim Q^{-1}$ and $\omega \sim Q^{-3/2}$ applies. That means, both functions intersect somewhere in the past, both frequencies must have had the same value then. The intersection point is at $Q = 1/2$, as we can see well at the lower frequent branch of PLANCK's radiation function being identical to the frequency response of an oscillating circuit with a Q-factor of $Q = 1/2$.

We just determined the frequency ω_0 extremely accurate. Thus, we also know $\omega_{0.5}$ very precise and reversely, we are able to calculate the frequency of the peak value of CMBR and with it, its temperature. Even the bandwidth of the LAPLACE-transform of the first maximum suggests a Q-factor of 0.5. This would correspond to the conditions at the point of time $t_1/4$ with $Q_{0.5} = 1/2$, $\omega_U = \omega_{0.5}$ as well as $r_1/2$, just our coupling-length. Then the frequency amounts to (new value):

$$\omega_{0.5} = \frac{1}{t_1} = \frac{2\kappa_0}{\epsilon_0} = \frac{\omega_1}{Q_{0.5}} = 2\omega_1 = 3.09408 \cdot 10^{104} \text{ s}^{-1} \quad (1)$$

That doesn't correspond to the value, which results from the impulse-length of the first maximum, but it is in the magnitude order. Now the conditions at this time are shaped by a very large uncertainty and a part of the emitted frequencies are, because of the large bandwidth, anyway above, others below (1), so that it is well possible that the in-coupling of the cosmologic background-radiation takes place right at this point of time with exactly this centre frequency.

The following contemplations for the in-coupling especially apply to the CMBR. Maybe it seems to be a little bit complicated, but it's just a model, which should reflect reality as well as possible, not the other way around. Now – up to the moment $t_1/4$ of input coupling, the already emitted energy exists as a free wave. The conditions at this point of time are analyzed in detail in Section 4.6.5.2. of [7] »The aperiodic borderline case«. Now there's going to be the construction of the metric lattice and the signal is coupled in. With the input coupling, a compression of the wavelength occurs i.e. an increase in frequency about the factor $\sqrt{2}$ due to a rotation of the coordinate system about 45° , which we have done in Section 4.3.4.3.3. of [7] (the metric wave moves in r-direction, the overlaid signals in x-direction).

Furthermore, the metric wave, as well as the energy to be coupled in, exist side by side up to the moment $t_1/4$, both with $\omega_0 \sim \omega_U \sim t^{-1/2} \sim Q_0^{-1}$. But with the in coupling $\omega_U \rightarrow \omega_s$ the temporal dependence changes into $\omega_s \sim t^{-3/4} \sim Q_0^{-3/2}$. This results in a transformation corresponding to a multiplication by a factor $2/3$, comparable with the transition from one medium to another with different refraction indices.

But there is yet another, additional effect: In Section 4.6.1. of [7] we found, that a cube with the edge length r_0 contains four MLE's altogether. Hence, the energy must be divided among these four MLE's. With it, the in-coupling frequency decreases additionally with the effect, that ω_s is smaller than $\omega_1/2$ now. The first two effects are depicted in Figure 1. The split we have to take into account elsewhere.

Altogether, to the frequency at the moment of in-coupling the following factor is applied $\omega_s = \frac{1}{4} \frac{2}{3} \sqrt{2} \omega_U = 2 \frac{1}{4} \frac{2}{3} \sqrt{2} \omega_1 = \sqrt{2}/3 \omega_1 \approx 0.4714 \omega_1 = 7.29281 \cdot 10^{103} \text{s}^{-1}$. With respect to the energy $\hbar_U \omega_U = 4 \hbar_1 \omega_1$ only a share of 94.28% incorporated, since \hbar is neither rotated, divided, nor transformed, it is a property of the metric wave field itself. The split has no effect onto the energy balance. The 94.28% relate to a coefficient of absorption of $\varepsilon_v = 0.9428 = \frac{2}{3} \sqrt{2}$. Therefore we are dealing with a *gray body* [4]. The *black body* is only a model, which doesn't exist in nature. The reflected share yields a further decrease of ω_s and with it even of ω_k . So we also have to multiply with ε_v .

Now to the transfer itself. According to (281 [6]) is the frequency of time-like vectors proportional to $\omega \sim t^{-3/4}$. That equals $\omega \sim Q^{-3/2}$ for the Q-factor. We do the following ansatz:

$$\omega_s = \frac{2 \cdot 1}{3 \cdot 4} \sqrt{2} \varepsilon_v \omega_{0.5} \left(\frac{Q_{0.5}}{Q_{0.5}} \right)^{\frac{3}{2}} = \frac{1}{6} \sqrt{2} \varepsilon_v \omega_U \left(\frac{1/2}{1/2} \right)^{\frac{3}{2}} = \frac{1}{6} \sqrt{2} \varepsilon_v \omega_U = \frac{1}{3} \sqrt{2} \varepsilon_v \omega_1 \quad (2)$$

$$\omega_k = \frac{2 \cdot 1}{3 \cdot 4} \sqrt{2} \varepsilon_v \omega_U \left(\frac{1/2}{Q_0} \right)^{\frac{3}{2}} = \frac{1}{6} \sqrt{2} \varepsilon_v \omega_U (2Q_0)^{-\frac{3}{2}} = \frac{1}{3} \sqrt{2} \varepsilon_v \omega_1 (2Q_0)^{-\frac{3}{2}} \quad (3)$$

$$z = \frac{\lambda_k - \lambda_s}{\lambda_s} = \frac{\omega_s}{\omega_k} - 1 \quad z + 1 = 2\sqrt{2} Q_0^{\frac{3}{2}} \quad z_{ab} = \begin{bmatrix} \frac{\omega_1}{\omega_k} & \frac{\hbar_1 \omega_1}{\hbar \omega_k} \\ \frac{\omega_U}{\omega_k} & \frac{\hbar_U \omega_U}{\hbar \omega_k} \end{bmatrix} = \frac{1}{\varepsilon_v} \begin{bmatrix} 6Q_0^{3/2} & 6Q_0^{5/2} \\ 12Q_0^{3/2} & 12Q_0^{5/2} \end{bmatrix}^* \quad (4)$$

$\frac{\omega_U}{\omega_s} = \frac{3}{\varepsilon_v} \sqrt{2} = 4.5$ *) Correct $m(Q_0^{3/2} - 1)$ resp. $m(Q_0^{3/2} - 1)Q_0$

The factor $2\sqrt{2}$ has nearly the same size as the factor $\tilde{x} = 2.8214$ from WIEN's displacement law. See Section 3. For the derivation. In Section 5. we will notice that using \tilde{x} instead of $2\sqrt{2}$, actually intended as an approximation, leads to the only result (136) that is within the error margins of the COBE measurement. Then (4) should read as follows:

$$z = \frac{\lambda_k - \lambda_s}{\lambda_s} = \frac{\omega_s}{\omega_k} - 1 \quad \left| \quad z + 1 = \tilde{x} Q_0^{\frac{3}{2}} \quad \left| \quad \varepsilon_v = \frac{\tilde{x}}{3} \quad \left| \quad \frac{\omega_U}{\omega_s} = \frac{9}{\tilde{x}} \sqrt{2} = 4.511145 \quad (5)$$

This would correspond to a slightly different refractive index and the factor \tilde{x} in (5) does not seem implausible either, as it is closely linked to the radiation laws. Apart from that we can see, that it's better to relate to ω_1 or ω_U . The components z_{1b} are describing the *frequency related*, the z_{2b} however the *energy related redshift*. For ω_k (5) we obtain a value of $1.00673 \cdot 10^{12} \text{s}^{-1}$. Curve 1 in Figure 2 corresponds to the signal ω_s redshifted by $\tilde{x} Q_0^{3/2}$ with the frequency response of a 1st order filter with the Q-factor $Q = 1/2$. Except for the decline in the upper frequency range it is identical with ω_k (Curve 6). The conditions before, during and after in-coupling are shown in Figure 1.

According to (5), the CMBR redshift has a value of $z = 6.79605 \cdot 10^{91}$, which is orders of magnitude higher than $z = 1100$, as »generally« assumed. On the one hand, this is due to the fact that this model works with variable natural »constants« whereas the photons behave like neutrinos shortly after BB and vice versa. Due to the expansion, i.e. the increase of $r_0 \sim Q_0$ (the viewer grows with it) the impression is given, that z is only proportional to $Q_0^{1/2}$. This would correspond to a value of $z = 8.14828 \cdot 10^{50}$ and is still well above 1100.

On the other hand, one assumes today that the physical laws shortly after BB did not differ significantly from those of today. So the origin of the CMBR is said to be around 3000 K, the recombination temperature of hydrogen, at a point in time 379000 years after BB. However, the exact results of the calculation of the CMBR temperature in relation to the time $t_{1/4}$ suggest that we must slowly get used to the idea that it must have been different at that time.

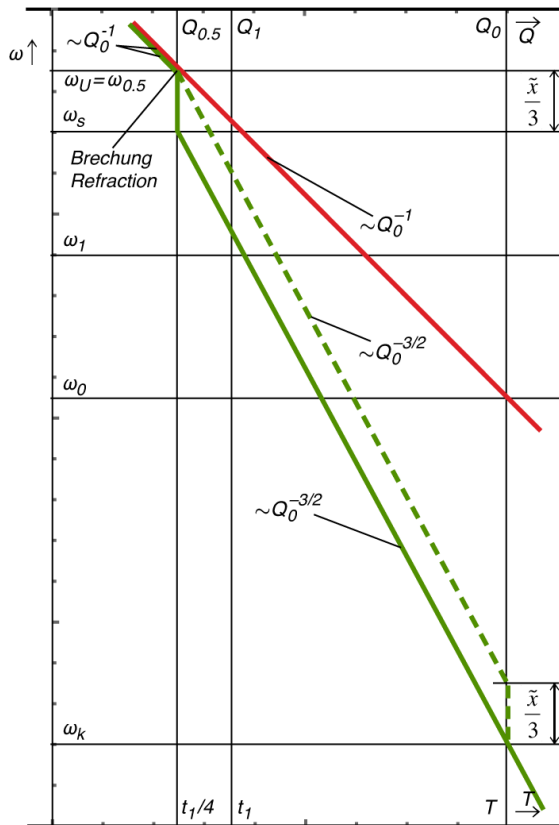


Figure 1
In-coupling process
and expansion

We have already realized that a single MLE owns an upper cut-off frequency (147 [7]), which changes during expansion. During propagation, only the active-part $A(\omega) \cdot \cos\phi_\gamma$ with $\phi_\gamma = B(\omega)$ is been transferred (real part). Thus we exactly get the value $\omega_g = 2\omega_1$, it applies $\Omega = \omega / (2\omega_1)$. With more exact contemplation we can see, the cut-off frequency may become effective in the first moments of propagation only.

Let's have a look at the moment of in-coupling now: The signal ω_s (curve 1) is multiplied with the frequency response $A(\omega) \cdot \cos\phi_\gamma$ after in-coupling. As a result, we obtain curve 2, which already comes very close to the PLANCK-curve. Now the signal is transferred to another MLE, at which point the frequency has decreased to a value of $\omega_s / \sqrt{2}$ within this period. We now re-apply the frequency response to the signal obtaining curve 3 (We considered the frequency to be constant at the presentation scaling up the upper cut-off-frequency accordingly instead). Curve 3 comes even closer to the targeted result. We repeat the entire process twice again obtaining graph 4 ($\omega_s / 1$) and finally graph 5 ($\omega_s / 2$), which figures a very good approximation of PLANCK's graph.

It could be so just thoroughly that PLANCK's radiation-law is really the result of the existence of an upper cut-off frequency of the vacuum. In this connection is to be paid attention to the fact, that that, being applied to time-like vectors emitted directly after Big Bang, must apply to each time-like vector emitted at a later point of time (e.g. today) too. With time-like vectors, it is impossible to determine exactly, when and where they have been emitted, they are timeless. Since no vector can be marked with respect to a second one, each thermal emission must run according to the same legalities (PLANCK's radiation-law) then.

After we have been able to confirm our assumption with the estimate, it is appropriate to carry out an exact calculation. We will do this in the next section.

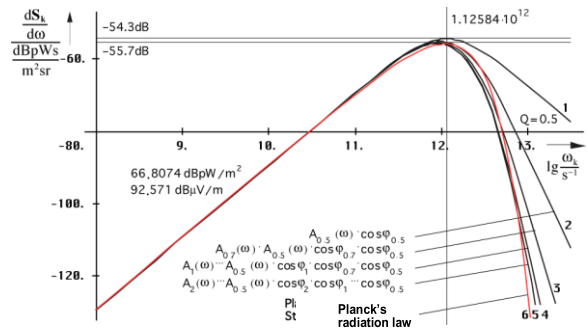


Figure 2
Intensity of the cosmologic
background radiation with estimate

Let us now assume that the decline at the higher frequencies is really caused by the existence of a cut-off frequency. In any case, such a specific course cannot be achieved with a normal LC-low-pass filter of any order. Then the intensity of the cosmological background radiation should have to follow exactly PLANCK's radiation formula. We therefore want to see whether PLANCK's curve 6 in Figure 2 can be approximated from the original curve 1, initially only as an estimate.

3. The WIEN displacement law and the source-function

During the examination of the WIEN displacement law meets the eye, that the displacement happens exactly at the lower wing pass of the PLANCK's radiation-function, which coincides with the wing pass of an oscillatory circuit with the Q-factor 1/2 in this section. Quite often in publications the curve is shown in another manner. I prefer the duplicate logarithmic presentation, then the curve turns into a straight line, which even clearly shows the function of the factor \tilde{x} , which makes the difference between peak and slope.

Considering the WIEN displacement law (13) more exactly, the factor $\tilde{x} = 2.821439372$ attracts attention particularly. With an oscillatory circuit of the Q-factor 1/2 rather the factor $2\sqrt{2}$ would be applicable for this, at which point the 2 stems from the source-frequency $2\omega_1$. The expression $\sqrt{2}$ arises from the rotation of the coordinate-system about $\pi/4$.

During an investigation in the Internet, I found a detailed deduction of the WIEN displacement law [2]. The value of the proportionality-factor can be obtained by the identification of the maximum of PLANCK's radiation law as follows. We start from (406 [7]):

$$dS_{\mathbf{k}} = \frac{1}{4\pi^2} \frac{\hbar\omega^3}{c^2} \frac{1}{e^{\frac{\hbar\omega}{kT}} - 1} \mathbf{e}_s d\omega \quad \text{PLANCK'S radiation law} \quad (406 [7])$$

$$dS_{\mathbf{k}} = \frac{1}{4\pi^2} \frac{k^3 T^3}{\hbar^2 c^2} \left(\frac{\hbar\omega}{kT}\right)^3 \frac{1}{e^{\frac{\hbar\omega}{kT}} - 1} \mathbf{e}_s d\omega \quad x = \frac{\hbar\omega}{kT} \quad d\omega = \frac{kT}{\hbar} dx \quad (6)$$

$$dS_{\mathbf{k}} = \frac{1}{4\pi^2} \frac{k^4 T^4}{\hbar^3 c^2} \frac{x^3}{e^x - 1} \mathbf{e}_s dx \quad \frac{d}{dx} \frac{x^3}{e^x - 1} = 0 \quad (7)$$

$$3 \frac{x^2}{e^x - 1} - \frac{x^3 e^x}{(e^x - 1)^2} = \frac{3x^2(e^x - 1) - x^3 e^x}{(e^x - 1)^2} = 0 \quad (8)$$

$$3x^2(e^x - 1) - x^3 e^x = 0 \quad x^3 e^x = 3x^2(e^x - 1) \quad (9)$$

$$e^x(x - 3) = -3 \quad y = x - 3 \quad x = 3 + y \quad (10)$$

$$ye^{y+3} = ye^y e^3 = -3 \quad ye^y = -3e^{-3} \quad (11)$$

$$x = 3 + \text{lx}(-3e^{-3}) = 2.821439372 \quad \text{lx}(xe^x) = x \quad (12)$$

lx is LAMBERT's W-function (ProductLog[#]). Finally, after insertion into the middle expression WIEN's displacement law turns out:

$$\hbar\omega_{\max} = \tilde{x} kT = 2.821439372 kT \quad \text{WIEN'S displacement law} \quad (13)$$

On success in doing the same even for the source-function with $Q=1/2$, obtaining the same result, we would be a step forward in answer to the question: Is the course of the Planck's radiation-function the result of the existence of an upper cut-off frequency of the vacuum? First of all however, we have to bring the output-function into a form, suitable for further processing. We start with ([7] 405) with the substitution:

$$P_v = \frac{P_s}{1 + v^2 Q^2} \quad v = \frac{\omega}{\omega_s} - \frac{\omega_s}{\omega} \quad \omega_s = 2\omega_1 \quad \Omega = \frac{\omega}{\omega_s} = \frac{1}{2} \frac{\omega}{\omega_1} \quad (14)$$

The expression stems from electrotechnics describing the power dissipation P_v of an oscillatory circuit with the Q-factor Q and the frequency ω (see [3]), v is the detuning. The Q-factor is known and amounts to $Q=1/2$ at $\omega_s=2\omega_1$. The right-hand expression results directly from the sampling-theorem. The cut-off frequency of the subspace ω_1 is the value ω_0 at $Q=1$. After substitution, we get the following expressions:

$$v = \Omega - \Omega^{-1} \quad v^2 = \Omega^2 + \Omega^{-2} - 2 \quad v^2 Q^2 = \frac{1}{4} \Omega^2 + \frac{1}{4} \Omega^{-2} - \frac{1}{2} \quad (15)$$

$$P_v = \frac{P_s}{\frac{1}{4} \Omega^2 + \frac{1}{4} \Omega^{-2} + \frac{1}{2}} \cdot \frac{4\Omega^2}{4\Omega^2} = 4P_s \frac{\Omega^2}{\Omega^4 + 2\Omega^2 + 1} = 4P_s \left(\frac{\Omega}{1 + \Omega^2} \right)^2 \quad (16)$$

You can find that expression more often in [1] and [7], among other things even with the group delay T_{Gr} however for a frequency ω_1 . For a frequency $2\omega_1$ applies for T_{Gr} and the energy W_v :

$$T_{Gr} = \frac{dB(\omega)}{d\omega} = \frac{1}{\omega_1} \left(\frac{\Omega}{1 + \Omega^2} \right)^2 \quad W_v = \frac{1}{6} P_s T_{Gr} = \frac{2}{3} \frac{P_s}{\omega_1} \left(\frac{\Omega}{1 + \Omega^2} \right)^2 \quad (17)$$

The factor $\frac{1}{6}$ comes from the splitting of energy onto 4 line-elements, as well as from the multiplication with the factor $\frac{2}{3}$ because of refraction during the in-coupling into the metric transport lattice. It often occurs in thermodynamic relations, which doesn't astonish. Thus, total-energy of the CMBR during input coupling is equal to the product of power dissipation and group delay, that is the average time, the wave stays within the MLE, but only for what it's worth. With the help of (16) we obtain:

$$P_v = 4b P_s \left(\frac{\Omega}{1 + \Omega^2} \right)^2 \quad P_v = 512b \hbar_1 \omega_1^2 \left(\frac{\Omega}{1 + \Omega^2} \right)^2 \quad (18)$$

b is a factor, we want to determine later on. Let's equate it to one at first. We determined the value P_s with the help of (394) using the values of the point of time $Q=1/2$. Interestingly enough, the HUBBLE-parameter H_0 at the time $t_{0.5}$ is greater than ω_1 and ω_0 . For an individual line-element applies:

$$\omega_{0.5} = \frac{\omega_1}{Q_{0.5}} = \frac{\omega_1}{\frac{1}{2}} = 2\omega_1 \quad H_{0.5} = \frac{\omega_1}{Q_{0.5}^2} = \frac{\omega_1}{\frac{1}{4}} = 4\omega_1 \quad (19)$$

$$P_s = \frac{\hat{h}_i}{4\pi t_{0.5}^2 Q_{0.5}^4} = \frac{\hat{h}_i}{2\pi} \frac{2^5}{4t_{0.5}^2} = 32\hat{h}_i H_{0.5}^2 = 128\hat{h}_i \omega_1^2 \quad \frac{\hat{h}_i}{2\pi} = \hbar_1 = \frac{\hbar_{0.5}}{2} \quad (20)$$

Expression (18) is very well-suited for the description of the conditions at the signal-source. Here, the power makes more sense than the POYNTING-vector \mathbf{S}_k . But for a comparison with (382) we just need an expression for \mathbf{S}_k , quasi a sort of PLANCK's radiation law for technical signals with the bandwidth $2\omega_1/Q_{0.5}=4\omega_1$. Then, this would look like this approximately:

$$d\mathbf{S}_k = 4bA \left(\frac{\Omega}{1 + \Omega^2} \right)^2 \mathbf{e}_s d\Omega \quad (21)$$

We determine the factor A by a comparison of coefficients (8). We assume, the WIEN displacement law (13) would apply and substitute as follows:

$$A = \frac{1}{4\pi^2} \frac{k^4 T^4}{\hbar^3 c^2} \quad c = \omega_1 Q^{-1} r_1 Q \quad (22)$$

We put in $2\sqrt{2}\omega_1$ as initial-frequency into the expression k^4T^4 . That's advantageous, as we will already see. This frequency is not a metric indeed ($\omega_x \sim Q^{-1}$), but an overlaid frequency ($\omega \sim Q^{-3/2}$). During red-shift of the source-signal, likewise not the factor 2.821439372 but the factor $2\sqrt{2}$ becomes effective. Thus applies:

$$k^4T^4 = \frac{(2\sqrt{2})^4}{(2\sqrt{2})^4} \hbar_1^4 Q^{-4} \omega_1^4 Q^{-6} = \hbar_1^4 \omega_1^4 Q^{-10} \quad Q^{-10} = \frac{Q^{-8}}{Q^2} \quad (23)$$

$$A = \frac{1}{4\pi^2} \frac{\hbar_1^4 \omega_1^4 Q^{-8}}{\hbar_1^3 Q^{-3} \omega_1^2 Q^{-2} r_1^2 Q^4} = \frac{1}{4\pi^2} \frac{\hbar^4 \omega_0^4}{\hbar^3 \omega_0^2 r_1^2 Q^4} = \frac{1}{\pi} \frac{\hbar \omega_0^2}{4\pi R^2} \quad (24)$$

$$4A = \frac{4}{\pi} \frac{\hbar \omega_0^2}{4\pi r_0^2 Q^2} = \frac{4}{\pi} \frac{\hbar \omega_0^2}{4\pi R^2} \quad R \text{ for } Q \gg 1 \quad (25)$$

$$dS_k = \frac{4b}{\pi} \frac{\hbar \omega_0^2}{4\pi R^2} \left(\frac{\Omega}{1+\Omega^2} \right)^2 \mathbf{e}_s d\Omega \quad R \text{ for } Q \gg 1 \quad (26)$$

Indeed, that submits only the expression without consideration of red-shift. We determine the actual values to the point of time of input coupling, in that we apply the values for $Q=1/2$ in turn. It applies:

$$A = \frac{1}{4\pi^2} \frac{\hbar_1^4 \omega_1^4 Q^{-8}}{\hbar_1^3 Q^{-3} \omega_1^2 Q^{-2} r_1^2 Q^4} = \frac{2^{8-3-2+4}}{4\pi^2} \frac{\hbar_1^4 \omega_1^4}{\hbar_1^3 \omega_1^2 r_1^2} = \frac{128}{\pi} \frac{\hbar \omega_1^2}{4\pi r_1^2} \quad (27)$$

$$4A = \frac{512}{\pi} \frac{\hbar \omega_1^2}{4\pi r_1^2} \quad dS_k = \frac{512b}{\pi} \frac{\hbar \omega_1^2}{4\pi r_1^2} Q^{-7} \left(\frac{\Omega}{1+\Omega^2} \right)^2 \mathbf{e}_s d\Omega \quad (28)$$

b will be determined later on. It shows, the POYNTING-vector is equal to the quotient of a power P_k resp. P_s and the surface of a sphere with the radius R (world-radius), exactly as per definition. Omitting the surface, we would get the transmitting-power P_v directly. In the above-mentioned expressions the parametric attenuation of $1Np/R$, which occurs during propagation in space, is unaccounted for. This must be considered separately if necessary.

Now we have framed the essential requirements and can dare the next step, the proof of the validity of the WIEN displacement law in strong gravitational-fields. The basic-idea was just, that the Planck's radiation law (382) should emerge as the result of the application of the metrics' cut-off frequency (302) to the function of power dissipation P_v of an oscillatory circuit with the Q -factor $Q=1/2$ (18). We proceed on the lines of (7), in that we equate the first derivative of the bracketed expression (28) to zero. A substitution like in (6) is not necessary, because the expression is already correct. It applies:

$$\frac{d}{d\Omega} \left(\frac{\Omega}{1+\Omega^2} \right)^2 = \frac{2\Omega}{(1+\Omega^2)^2} - \frac{4\Omega^3}{(1+\Omega^2)^3} = \frac{2\Omega(1-\Omega^2)}{(1+\Omega^2)^3} = 0 \quad (29)$$

$$2\Omega(1-\Omega^2) = 0 \quad \Omega_1 = 0 \quad \text{Minimum} \quad \Omega_{2,3} = \pm 1 \quad \text{Maximum} \quad (30)$$

The first solution is trivial, the second and third is identical, if we tolerate negative frequencies (incoming and outgoing vector). Now, we must only find a substitution for Ω , with which (382) and (28) come to congruence in the lower range. This would be the displacement law for the source-signal then (27). Since the ascend of both functions has the same size in the lower range, there is theoretically an infinite number of superpositions, whereat only one of them is useful. Therefore, as another criterion, we introduce, that both

maxima should be settled at the same frequency. The displacement law for the source-signal would be then as follows:

$$\hbar\omega_{\max} = a kT \quad \text{Displacement law source-signal} \quad (31)$$

at which point we still need to determine the factor a. As turns out, we still have to multiply even the output-function itself, with a certain factor b, in order to achieve a congruence. The 4 we had already pulled out. We apply the value $2\sqrt{2}$ and 2.821439372 for a one after the other and determine b numerically with the help of the relation and the function FindRoot[#] using the substitution $2x=ay$:

$$\frac{\left(a \frac{y}{2}\right)^3}{e^{a \frac{y}{2}} - 1} - 4b \left(\frac{\frac{y}{2}}{1 + \left(\frac{y}{2}\right)^2}\right)^2 = 0 \quad y=10^{-5} \quad \begin{array}{ll} b \rightarrow 2 & \text{for } a=2\sqrt{2} \\ b \rightarrow 2.009918917 & \text{for } a=2.821439372 \end{array} \quad (32)$$

The maxima overlap accurately in both cases. The lower value a is equal to the factor in (903). Thus it seems, that with references, except for those to the origin of each wave with $2\omega_1$, multiplied with $\sqrt{2}$, which is caused by the rotation of the coordinate-system about $\pi/4$, rather the approximative solutions with the factor $2\sqrt{2}$ apply. With lower frequencies, the factor 2.821439372 of the WIEN displacement law applies then again.

But to the exact proof of the validity of the WIEN displacement law in the presence of strong gravitational-fields this ansatz is not enough. We must also show that the maximum of the PLANCK's radiation-function behaves exactly according to the WIEN displacement law, that means the approximation and the target-function must come accurately to the congruence. Since the difference between a factor $2\sqrt{2}$ and 2.821439372 amounts to 0.5% after all, we will execute the examination with both values. Only the relations for $b=2\sqrt{2}$ are depicted. Now, we can set about to write down the individual relations:

$$\hbar\omega_{\max} = 2\sqrt{2} kT \quad \text{Displacement law source-signal} \quad (33)$$

$$\Omega = \frac{1}{2} \frac{\omega}{\omega_1} = \frac{1}{2\sqrt{2}} \frac{\hbar\omega}{kT_k} = \frac{x}{a} = \frac{y}{2} \quad y = \frac{\omega}{\omega_1} \quad b=2 \quad (34)$$

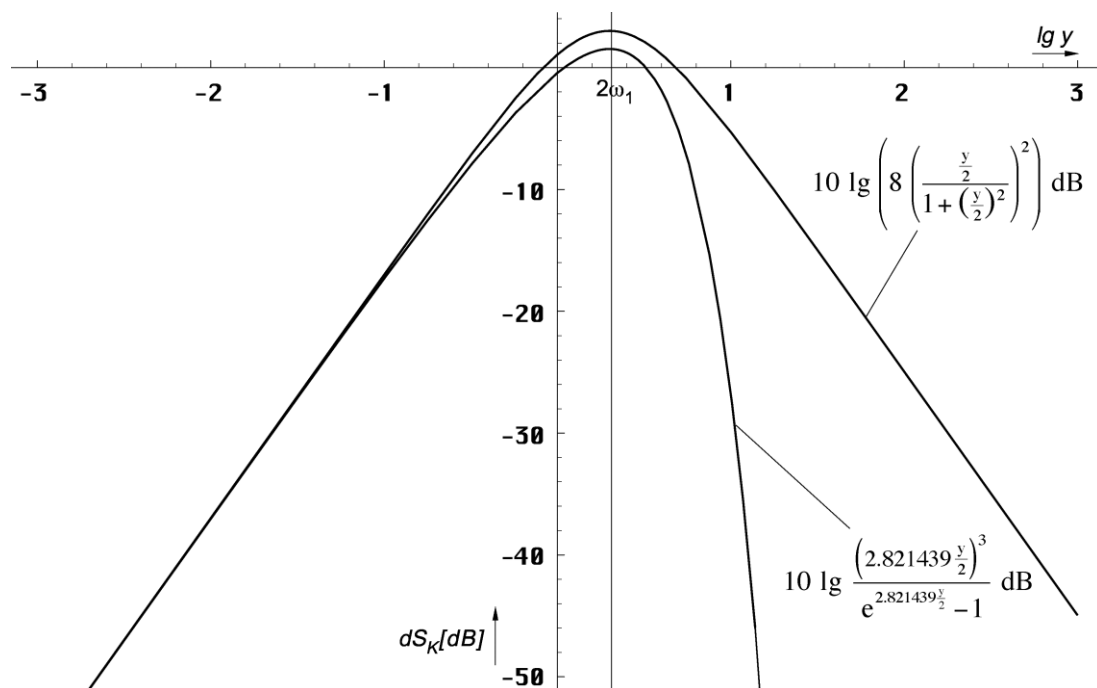


Figure 3
Planck's radiation law and source-function
in the superposition (logarithmic, relative level)

Thus, we have found our source-function. In y it reads as follows:

$$dS_k = \frac{16}{\pi} \frac{\hbar\omega_0^2}{4\pi R^2} \left(\frac{\frac{y}{2}}{1 + \left(\frac{y}{2}\right)^2} \right)^2 e_s dy \quad R \text{ for } Q \gg 1 \quad (35)$$

But we aren't interested in the absolute value but in the relative level only:

$$dS_1 = 8 \left(\frac{\frac{y}{2}}{1 + \left(\frac{y}{2}\right)^2} \right)^2 dy \quad (36)$$

We want to mark the approximation with dS_2 . For the target-function dS_3 we obtain:

$$dS_3 = \frac{(2.821439 \frac{y}{2})^3}{e^{2.821439 \frac{y}{2}} - 1} dy \quad (37)$$

The course of the source-function and the PLANCK's graph are presented in Figure 3.

4. Solution and analysis

Of course, there is no shift-information $y(Q)$ contained in these relations. Since the considered system is a minimum phase system, we now have to multiply the source-function dS_1 with the amplitude response $A(\omega)$. The result is our approximation dS_2 . It is merely applied to a single line-element, which is traversed by the signal in the time r_0/c . Thereat r_0 is equal to the PLANCK's length and identical to the wavelength of the above-mentioned metric wave-function. That means, we have to execute the multiplication with $A(\omega)$ as often as we like, unless the result (almost) no longer changes.

But thereat as well the frequency of the source-function as the cut-off frequency (frequency response) decrease continuously. Therefore it's opportune, to take up the displacement (frequency and amplitude) later on with the result dS_2 (approximation), instead of shifting on and on the location of the source-function. For the proof of our hypothesis indeed this last shift is not of interest, so that we won't take up it in this place.

There is another problem with the amplitude response $A(\omega)$ and with the phase-angle φ . Since the cut-off frequency $\omega_0 = f(Q, \omega_1)$ and the frequency ω are varying according to different functions, it causes difficulties to formulate a practicable algorithm. Thus we use the fact that there is no difference, whether we reduce the frequency of the input-function with constant cut-off frequency or if we shift upward the cut-off frequency with constant input-frequency. But this corresponds to a *transposition of integration limits*. We choose this second way incl. the displacement of the approximation at the end of calculation. This all the more, since we would be concerned with two time-dependent quantities (input-frequency and cut-off frequency) otherwise. To the approximation applies:

$$dS_2 = 8 \left(\frac{\frac{y}{2}}{1 + \left(\frac{y}{2}\right)^2} \right)^2 \overset{\frac{1}{2}}{\int}_{Q_0} A(y) \cos \varphi(y) \bar{d}y dy \quad (38)$$

Expression (33) looks a little bit strange maybe. It's about a so called product integral, i.e. you have to multiply instead of summate. Then, the letter \bar{d} isn't the differential-, but the... let's call it *divisional-operator*. I don't want to amplify that, because we anyway have to convert expression (33) to continue. We use $Q_0 = 8.34047113224285 \cdot 10^{60}$ from [6] as the updated value of the Q-factor and the phase-angle of the metric wave-function¹. It determines

¹ The equality of the Q-factor Q_0 and the phase angle $2\omega_0 t$ is a special property of this function

the upper limit of the multiplication resp. summation. Fortunately the frequency response can be depicted as e-function, so that the product changes into a sum. We simply have to integrate the exponent quite normally then. We obtain the frequency response inclusive phase-correction with the help of the complex transfer-function (150) to:

$$A(\omega) \cdot \cos\varphi(\omega) = e^{\Psi(\omega)} \quad \varphi = B(\omega) \quad \text{Frequency response of a line element} \quad (39)$$

The fact, that only the real component is transferred, is taken into account by the multiplication of $A(\omega)$ with the expression $\cos\varphi$. I used (302) from [1] for $\Psi(\omega)$. Unfortunately, the expression stated there is wrong, because I miscalculated in Section 4.3.2. and I could reveal the error only now. After all the function determined there was not referenced in any correspondence table and I was unable to perform the inverse Laplace-transform to the verification until then.

The corrected expressions and figures have been published in [7] as well as in a corrigendum. Fortunately I used a different approach for the rest of the work, without an error. Only Section 4.3.2. was concerned. With $\omega_1 = 1/(2t_1) = \kappa_0/\varepsilon_0$ expression (140 [1]) reads correctly:

$$y(p) = e^{\int \frac{a-p}{p^2} dp} = \frac{C_1}{p} e^{-\frac{a}{p}} = \frac{a}{p} e^{-\frac{a}{p}+c} = \frac{1}{2pt_1} e^{-\frac{1}{2pt_1}+c} \quad (140 [7])$$

Because of $\cos(\varphi) = \cos(-\varphi)$ we obtain the following corrected expression (302 [1]):

$$\Psi(\omega) = -\frac{1}{2} \ln(1+\Omega^2) + \frac{\Omega^2}{1+\Omega^2} + \ln \cos\left(\arctan \Omega - \frac{\Omega}{1+\Omega^2}\right) \quad (305 [7])$$

As next, we substitute Ω by y with the help of (34):

$$\Psi(\omega) = -\frac{1}{2} \ln\left(1 + \left(\frac{y}{2}\right)^2\right) + \frac{\left(\frac{y}{2}\right)^2}{1 + \left(\frac{y}{2}\right)^2} + \ln \cos\left(\arctan \frac{y}{2} - \frac{\frac{y}{2}}{1 + \left(\frac{y}{2}\right)^2}\right) \quad (40)$$

The value ω in the numerator of y figures the respective frequency of the cosmic background-radiation, for which we just want to determine the amplitude. It is identical to the ω in PLANCK's radiation law. Thereat, it's about an overlaid frequency, which is proportional to $Q^{-3/2}$ in the approximation. The frequency ω_0 is exactly proportional to Q^{-1} .

Instead of the value ω_1 in the denominator actually the PLANCK's frequency ω_0 should be written with the frequency response. That is also the cut-off frequency for the transfer from one line-element to another. But with $Q=1$ the value ω_0 is right equal to ω_1 , at which point ω_0 varies with the time; ω_1 on the other hand is strictly defined by quantities of subspace having an invariable value therefore. It applies $\omega_0 = \omega_1/Q$. That means, that even y depends on time, being proportional to $Q^{-1/2}$.

Now however, we want to freeze the value ω , at least up to the end of the calculation, with the consequence, that we must divide y by a supplementary function ξ , which is proportional to $Q^{1/2}$. It applies $\xi = cQ^{1/2}$ and

$$\Psi(\omega) = -\frac{1}{2} \ln\left(1 + \left(\frac{y}{2\xi}\right)^2\right) + \frac{\left(\frac{y}{2\xi}\right)^2}{1 + \left(\frac{y}{2\xi}\right)^2} + \ln \cos\left(\arctan \frac{y}{2\xi} - \frac{\frac{y}{2\xi}}{1 + \left(\frac{y}{2\xi}\right)^2}\right) \quad (41)$$

The factor c arises from the initial conditions at $Q=1/2$ (resonance-frequency $2\omega_1$, cut-off frequency ω_1) to $c=4$ (In the program $cc=y/2$):

$$y = \frac{\omega}{\omega_0} \sim \frac{2^{-3/2}}{2^{1/2}} = \frac{1}{4} \quad \xi = 4\sqrt{Q} \quad \text{Approximation} \quad (42)$$

Thus, together with the 2 of $y/2$, we acquire exactly the same factor 8 as in the source-function (36). Then, the approximation dS_2 calculates as follows:

$$dS_2 = 8 \left(\frac{\frac{y}{2}}{1 + \left(\frac{y}{2}\right)^2} \right)^2 e^{-\int_{1/2}^{Q_0} \frac{1}{2} \ln \left(1 + \left(\frac{y/2}{\xi} \right)^2 \right) + \frac{y/2}{1 + \frac{y/2}{\xi}} + \frac{1}{2} \ln \cos \left(\arctan \frac{y/2}{\xi} - \frac{y/2}{1 + \frac{y/2}{\xi}} \right)} dy \quad (43)$$

The negative sign before the integral results from the re-exchange of the integration limits. For the determination of the integral, a value of 10^3 as upper limit suffices indeed. Over and above this, it changes very little. Therefore, I worked with an upper limit of $3 \cdot 10^3$ in the following representations. The integral only can be determined numerically, namely with the help of the function `NIntegrate[f(Q), Q, 1/2, 3×103]`. The quotient of $y/2$ and ξ expression (42) however describes the dependency $y(Q)$ in the approximation only. There is an exact solution as well. According to [1] (209), (299) and (509) applies:

$$\xi = \frac{a}{b} \frac{1}{Q} \frac{R(Q)}{R(\tilde{Q})} \frac{\sqrt{\beta_\gamma^4 - 1}}{\sqrt{\tilde{\beta}_\gamma^4 - 1}} \quad \text{with } \tilde{Q} = \frac{1}{2} \quad \text{and} \quad (44)$$

$$R(Q) = \frac{3}{2} Q^{\frac{1}{2}} \int_0^Q \frac{dQ}{\rho_0} \quad \text{with } \rho_0 = \frac{1}{2} \sqrt[4]{(1 - A^2 + B^2) + (2AB)^2} \quad (45)$$

$$A = \frac{J_0(Q)J_2(Q) + Y_0(Q)Y_2(Q)}{J_0^2(Q) + Y_0^2(Q)} \quad B = \frac{J_2(Q)Y_0(Q) - J_0(Q)Y_2(Q)}{J_0^2(Q) + Y_0^2(Q)} \quad (46)$$

The factor b arises from the demand, that the exact function ξ and its approximation should be of the same size with larger values of Q . The factor a we will determine later on in turn. The functions in (46) are Bessel functions.

Problematic in (45) and (50) is the integral, which can be determined even only by numerical methods. In order to avoid the numerical calculation of an integral within the numerical calculation of another integral, it's opportune, to replace the integrand by an interpolation-function (BRQ1), and that inclusive the factor B . The value r_1 cancels itself because of (44). We choose sampling points with logarithmic spacing:

```
brq = {{0, 0}};
For[x = -8; i = 0, x < 25, (++i), x += .1;
  AppendTo[brq, {10^x, N[BRQP[10^x]/BGN/(2.5070314770581117*10^x) ]}]]
BRQ0 = Interpolation[brq];
BRQ1 = Function[If[# < 10^15, BRQ0[#], Sqrt[#]]];
(47)
```

The function BRQP is equal to the product of Q , root-expression and integral in the denominator of (50). The value BGN is equal to the initial value of the same product at $Q=1/2$. You'll find the complete program in the appendix. The factor b arises to 2.5(0703). According to (214 [7]), (581 [7]) and (623 [7]) applies further:

$$\beta_\gamma = \frac{\sin \alpha}{\sin \gamma_\gamma} \quad \gamma_\gamma = \arg \underline{c} + \arccos \left(\frac{c_M}{c} \sin \alpha \right) + \frac{\pi}{4} \quad (48)$$

$$\alpha = \frac{\pi}{4} - \arg \underline{c} = \frac{3}{4} \pi + \frac{1}{2} \arg \left((1 - A^2 + B^2) + j2AB \right) \quad c_M = |\underline{c}| \quad (49)$$

$$\xi = \frac{3}{0.56408} \frac{a}{b} Q^{-\frac{1}{2}} \sqrt{\beta_\gamma^4 - 1} \int_0^Q \frac{dQ}{\rho_0} = a \frac{3}{2} \sqrt{2} Q^{-\frac{1}{2}} \sqrt{\beta_\gamma^4 - 1} \int_0^Q \frac{dQ}{\rho_0} \quad (50)$$

\underline{c} is the complex propagation-velocity of the metric wave-field. As next, we want to take up a comparison of the two functions $Q^{1/2}$ and BRQ1 (Figure 4):

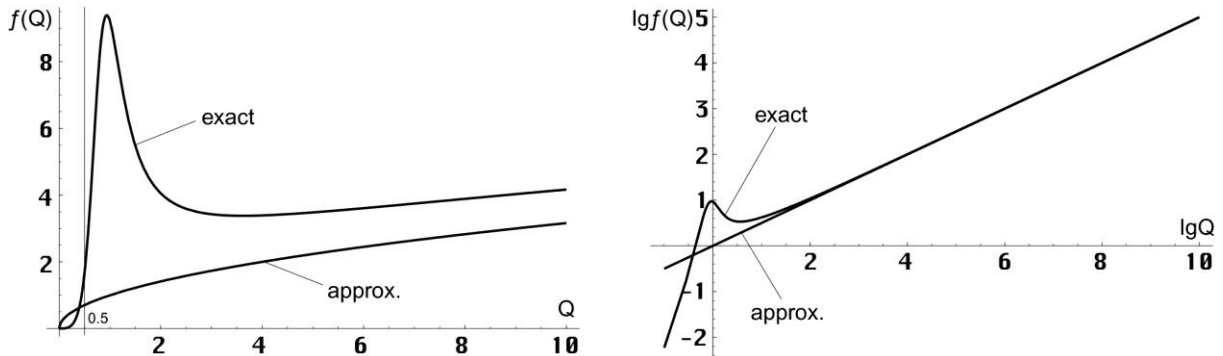


Figure 4
Function BRQ1 exactly and approximation

On the basis of the demand, that the result of both functions must be identical with $Q \gg 1$ we choose the factor a to $\sqrt{\pi}$. In this connection is to be remarked that the exact value is $\sqrt{3,5}$ in fact. But since we finally will not find, in any case, an exact fit in the course of both functions, this small „cheating“ in the initial conditions should be allowed. The value $\sqrt{\pi}$ namely leads to the result with the smallest difference, so that we obtain the following final relation for ξ :

$$\xi = \frac{3}{2} \sqrt{2\pi} \left(Q^{-\frac{1}{2}} \sqrt{\beta_\gamma^4 - 1} \int_0^Q \frac{dQ}{\rho_0} \right) \quad cc = \frac{3}{2} \sqrt{2\pi} = 3.756 \quad (51)$$

For $\sqrt{3,5}$ a value of $c=4$ would arise. The bracketed expression corresponds to the factor $Q^{1/2}$ in the approximation. The course of the integral function in (43) as well as of the dynamic cumulative frequency response $A_{ges}(\omega) = e^{-\int \Psi(\omega) dQ}$ you can see in Figure 5 and 6. For your information the amount of the complex frequency response $|X_n(j\omega)|$ of subspace is plotted, that's the medium, in which the metric wave field propagates ($\Omega_U = \Omega$).

$$X_n(j\omega) = \frac{1}{2} \frac{1}{1+j\Omega} \left(1 + \frac{1}{1+j\Omega} \right) \quad \text{Complex spectral function} \quad (52)$$

That applies to EM-waves propagating simultaneously with the metric wave field but not to the metric wave field itself. They achieve the aperiodic borderline case at $Q=1/2$.

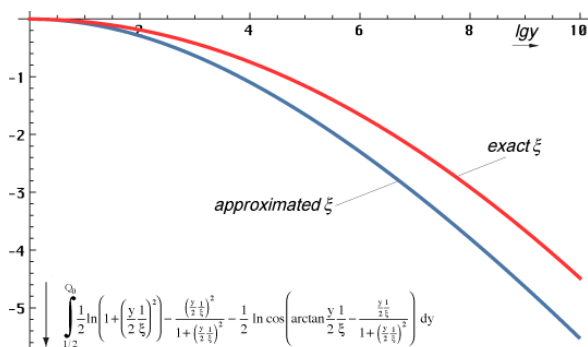


Figure 5
Course of the Integrals $\Psi(\omega)$ in (43) for the approximation and exact function ξ

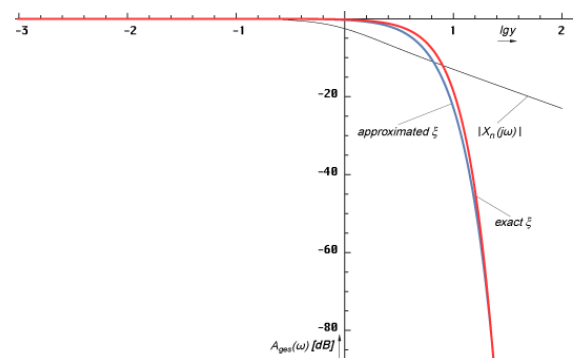


Figure 6
Cumulative frequency response $A_{ges}(\omega)$ and $|X_n(j\omega)|$ of the metric wave field and subspace

Thus, all requirements are filled and we are able to demonstrate the course of the approximation (43) in comparison with the target-function (37) and that as well for the approximation as for the exact function ξ . We use a logarithmic scale with the unit decibel [dB] and, because it's about power per surface, with the factor 10.

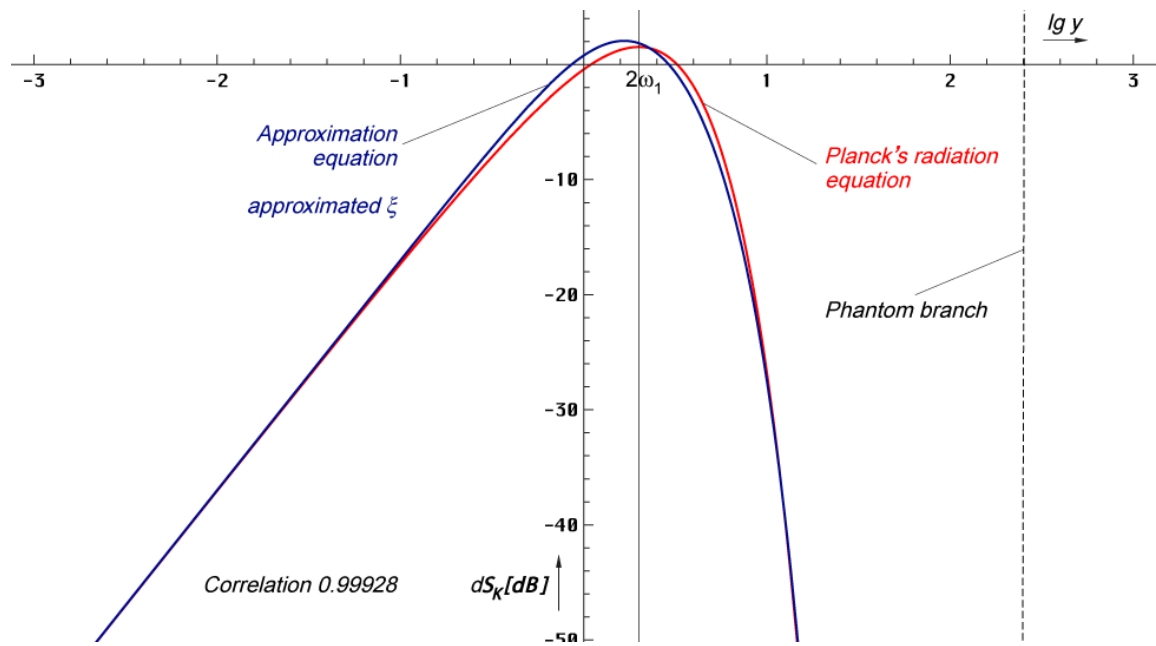


Figure 7
 PLANCK's radiation law and approximation
 with approximation for the function ξ (relative level)

Figure 7 shows the shape of the approximation using the approximation (42) for the function ξ ($c=4$). The figure shows a phantom branch at the right side due to the down-limited decimal resolution by sign-change according to $e^{1/\pm \rightarrow 0}$. It will be removed in the following presentations. Furthermore we can see, both curves doesn't match exactly. The maximum frequency Ω_{th} is downshifted by 18.28% (0.81721). The maximum deviation of the amplitude ΔA_{π} is with -1.78dB , the difference between both maxima $\Delta A_{\pi} +0.42886\text{dB}$ ($+10.38\%$ resp. 1.1038). Altogether the function resembles the shape, shown in [7] Section 4.6.4.2.3., obtained by multiplication of the source-function with only 4 choosed values of the frequency response. But there are disparities in the declining branch with higher frequencies.

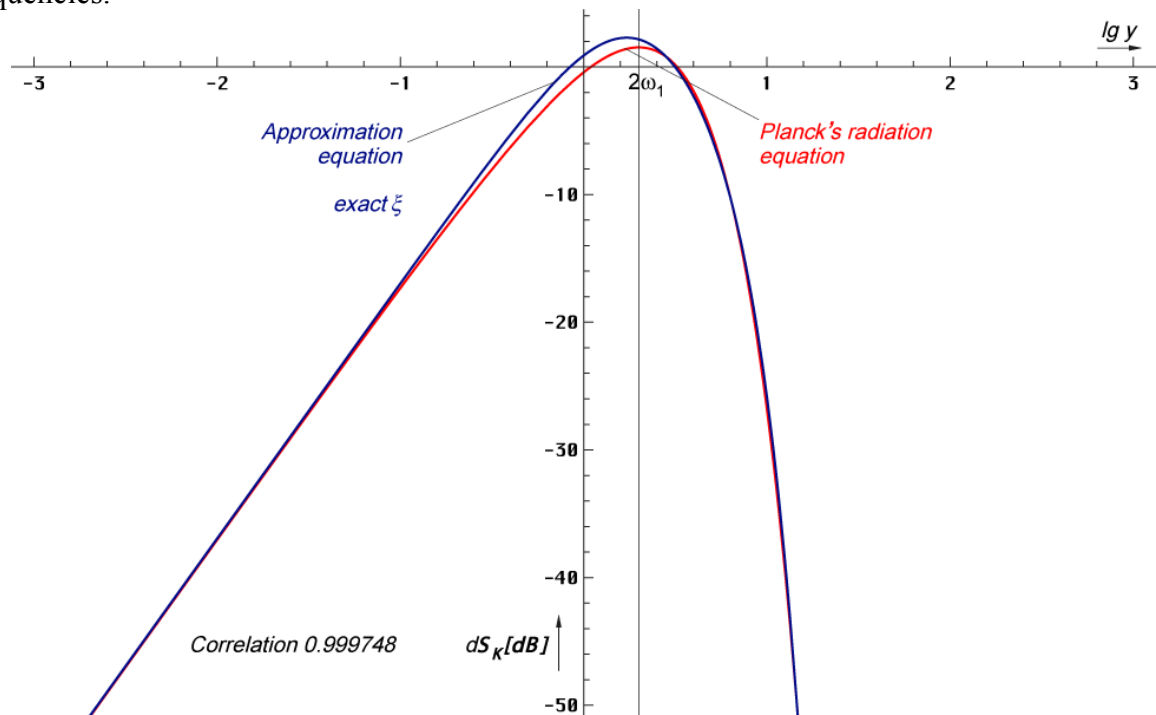


Figure 8
 PLANCK's radiation law and approximation under
 application of the exact function ξ (relative level)

Figure 8 presents the course of the approximation under application of the exact function ξ (51) for $c=3.756$. With it, the best fit (without group delay correction) turns out (With $c=4$, there is only a minor difference to Figure 7). But both functions don't overlap exactly neither in this place. Once again, the maximum frequency Ω_{th} is downshifted by 13.61% (0.86386). The maximum deviation of amplitude ΔA_{π} is about +1.33 dB, between both maxima ΔA_{π} at +0.75834 dB (+19.07%).

The course of deviation (logarithm of the quotient of approximation and PLANCK's radiation law) as a function of y is shown in Figure 9. One sees, from ca. $10\omega_1$ on the relative deviation between both functions is strongly growing. But since the absolute level in this range is already microscopic (-54dB at the third zero), nobody will take notice of it. Even there it seems rather to be about a small frequency shift, than about a deformation of the envelope.

In any case, the form of the approximation-graph doesn't correspond to that of a black emitter and the value is too high. But during the COBE-experiment, they just have been ascertained, that the spectrum of the CMBR is exactly? black. Therefore, more forces are required in order to change the form in such a manner, that it equals that of a black emitter. In the next section we will see, which influences may come into consideration for that purpose.

As further considerations [6] show, the above mentioned deviation is less because of the curve shape, but because of the value of the HUBBLE-parameter, determined in [1]. With the value from [6] and [7] the calculation exactly fits the limits of the measuring tolerance of the COBE/WMAP-satellite. Read Section 5 for details.

In Figure 9 we can see that we yield an improvement if we use the exact function ξ . Nevertheless a certain left-over difference remains. If we take a look at the course in the 2nd quadrant, we can see a „gap“ where an already known function, multiplied with the factor $\frac{1}{2}$, could slot right in there.

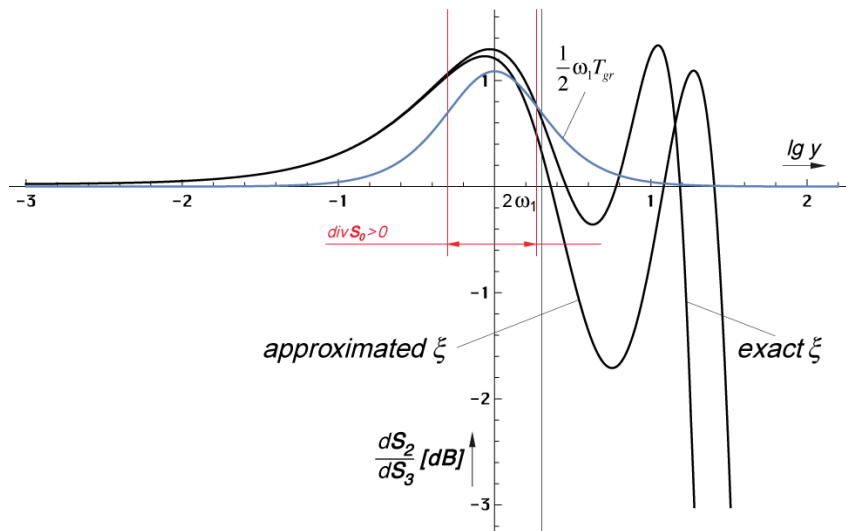


Figure 9
Relative offset between approximation and radiation law in dependency of the function ξ used

That's the group delay T_{Gr} of the metric wave field of [7] Section 4.3.2. Whereas the phase response affects the form of the carrier frequency (ω_1 resp. ω_0), the group response affects the shape of the envelope curve. It reads:

$$T_{\text{Gr}} = \frac{d}{d\omega} B(\omega) = -\frac{2}{\omega_1} \left(\frac{\Omega}{1+\Omega^2} \right)^2 = -2 \frac{\theta^2}{\omega_1} \quad (53)$$

With $\Omega=\omega/\omega_1$. The factor 2 cancels out, since it's about a spin2-system, with which all temporal constants are $2T$ instead of T (double phase-/group-velocity). Whereas the group response is constantly equal to zero across nearly all decades, it is not the case close to ω_1 resp. ω_0 nowadays. A frequency dependent group response always leads to a distortion of the envelope curve.

As we can see, the group response is negative. That happens in technology too and is not a violation of causality. See [8] for details. So far we have taken into account the frequency response $A(\omega)$ and the phase response $B(\omega)$, only the group delay correction $\Theta(\omega) = \frac{1}{2}\omega_1 T_{gr}$, is missing, implemented by the function $gdc[\omega]$:

$$\frac{1}{2}\omega_1 T_{Gr} = -\frac{2\omega_1}{2\omega_1} \left(\frac{\Omega}{1+\Omega^2} \right)^2 = -\left(\frac{\Omega}{1+\Omega^2} \right)^2 \quad (54)$$

$$\Theta(\omega) = e^{-\omega T_{Gr}} = e^{-\left(\frac{\Omega}{1+\Omega^2}\right)^2} = 10^{-\left(\frac{\Omega}{1+\Omega^2}\right)^2 \lg e} = 10^{-0,434294 \left(\frac{\Omega}{1+\Omega^2}\right)^2} \quad (55)$$

The decimal power is important, if we want to calculate with dB. The group delay correction $\Theta(\omega)$ on dS_2 is applied only once:

$$dS_2 = 8 \left(\frac{\frac{y}{2}}{1+\left(\frac{y}{2}\right)^2} \right)^2 e^{\int_{1/2}^{Q_0} \frac{1}{2} \ln \left(1 + \left(\frac{y/2}{2\xi} \right)^2 \right) - \frac{y/2}{1+\frac{y/2}{2\xi}} - \frac{1}{2} \ln \cos \left(\arctan \frac{y/2}{2\xi} - \frac{y/2}{1+\frac{y/2}{2\xi}} \right) dy} - \frac{1}{2}\omega_1 T_{Gr} \quad dy \quad (56)$$

The resulting functions with group delay correction for both ξ are shown in Figure 10 and 11. There is already a better fit of both graphs in Figure 10, as we can see. Now the maximum Ω_m of the frequency is downshifted about 12.52% (0.87476). The maximum deviation of amplitude ΔA_π amounts to +0.42061 dB. The deviation between both peaks ΔA_π is -0.40484 dB or -1.45%.

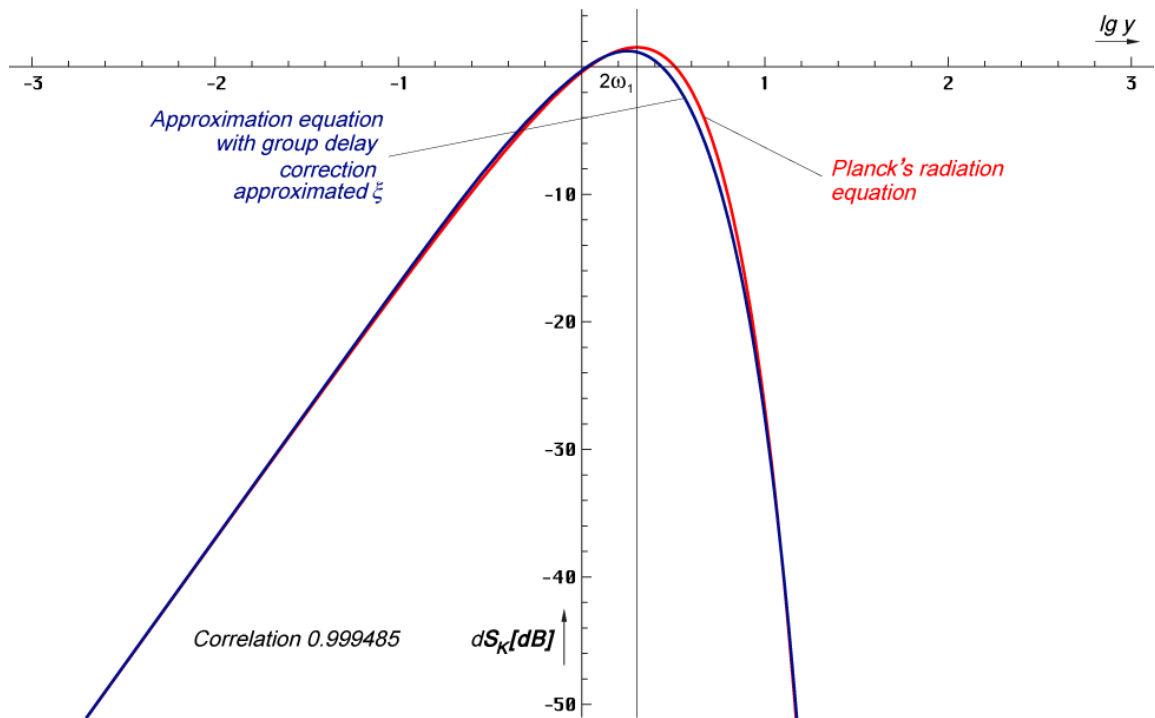


Figure 10
PLANCK's radiation law and approximation with group delay correction with approximation of the function ξ (relative level)

A nearly perfect result we have got for the case exact ξ with group delay correction (Figure 11). Now the maximum frequency Ω_m is downshifted about -7.00% (0.93003) only. That value is far in excess of the -2.36% deviation between measured and calculated CMBR-temperature. The maximum amplitude deviation ΔA_π is at about -0.58954 dB, between both maxima ΔA_π is at -0.02762 dB (-0.64%). Of particular interest is the extremely high correlation coefficient of 0.999835 between both curves.

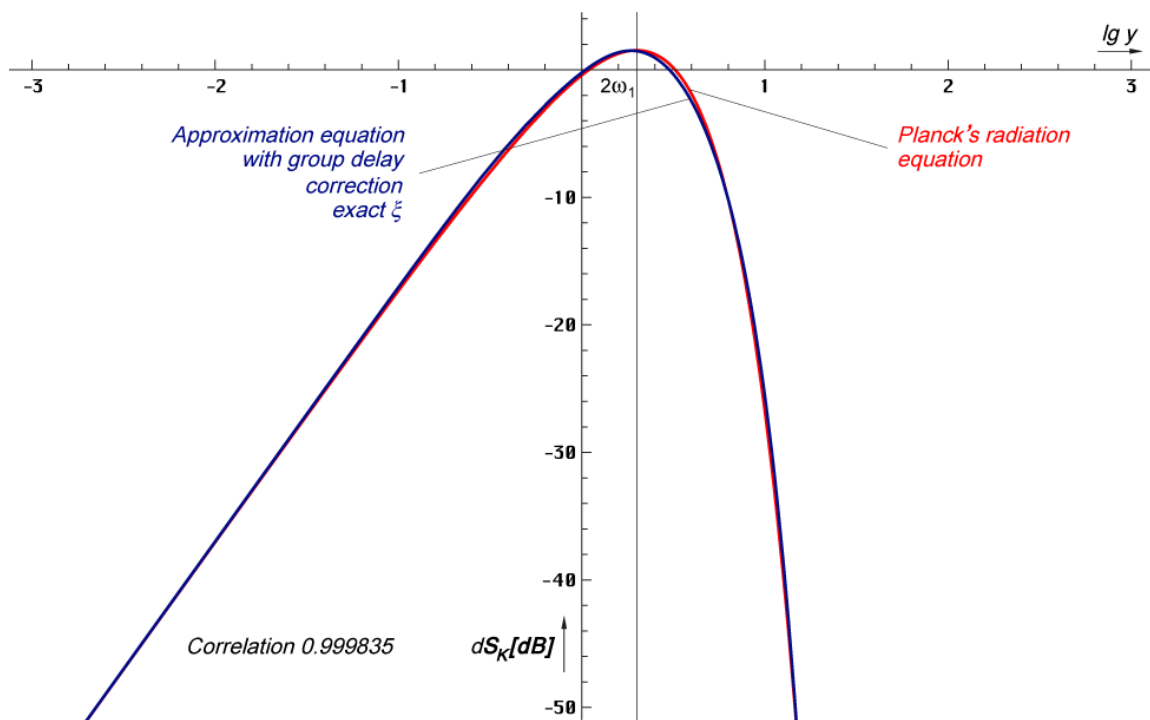


Figure 11
 PLANCK'S radiation law and approximation with group delay correction under application of the exact function ξ (relative level)

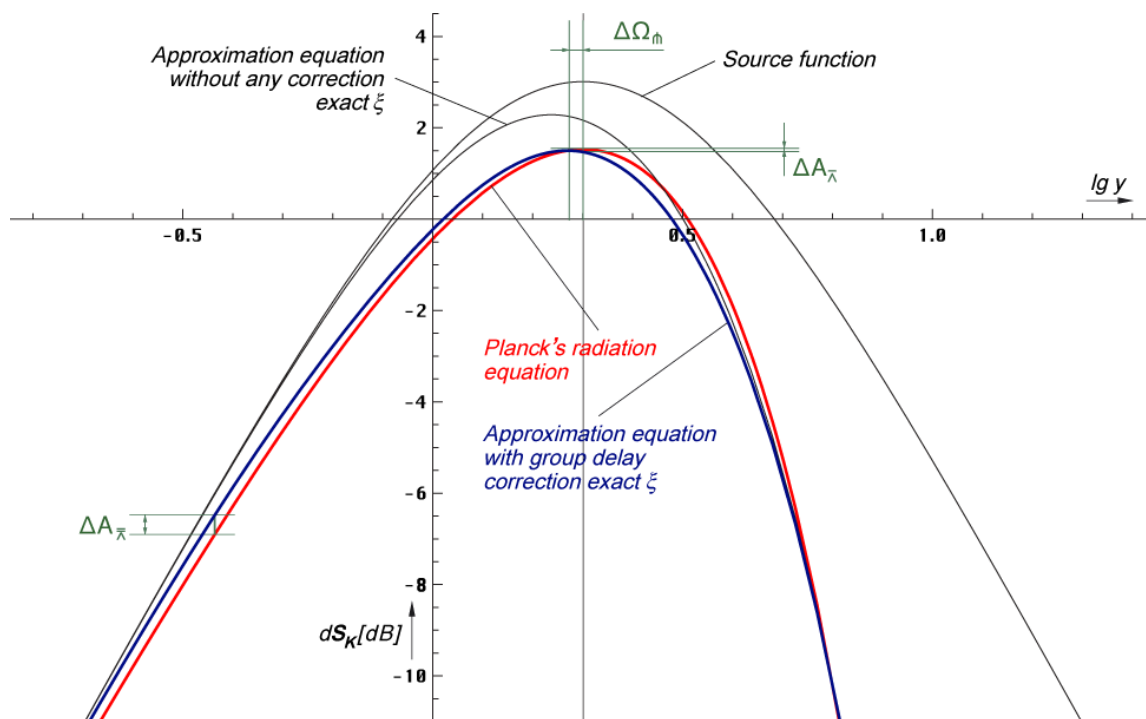


Figure 12
 PLANCK'S radiation law and approximation with group delay correction under application of the exact function ξ (relative level) high resolution

To the better clarity, the last case is depicted in Figure 12 with higher resolution. You can find the exact results in Table 1. Figure 13 shows a summary of the relative deviations of all solutions in comparison with the course of the absolute value of the complex frequency response $|X_n(j\omega)|$ of subspace.

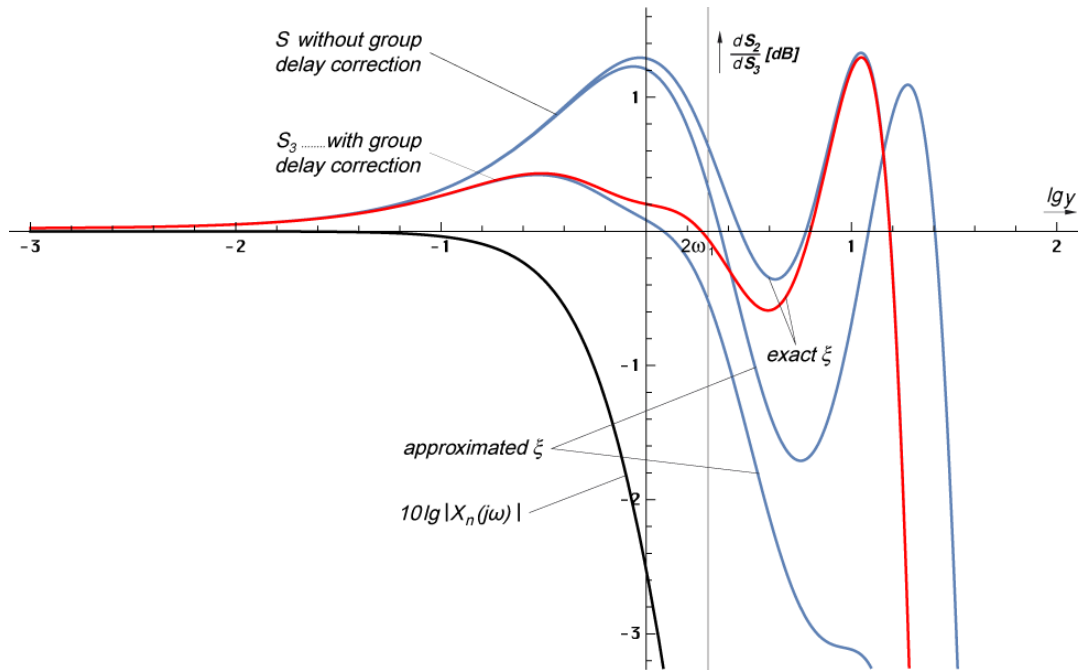


Figure 13
Relative deviation between approximation and radiation law according to the function ξ used without and with group delay correction

Value	Ω_{m}	$\Delta\Omega_{\text{m}}$	A_{π}	ΔA_{π}	Ω_{π}	ΔA_{π}	Ω_{π}	ΔA_{π}
	[1]	[%]	[dB]	[dB]	[1]	[dB]	[1]	[dB]
Planck	1.00000	± 0.00	+1.52727	± 0.00000	--	--	--	--
Figure 7	0.81721	-18.28	+1.95613	+0.42886	0.41944	+1.20008	2.88334	-1.78499
Figure 8	0.86386	-13.61	+2.28561	+0.75834	0.46495	+1.29392	5.55922	+1.32996
Figure 10	0.87476	-12.52	+1.12244	-0.40484	0.14776	+0.42061	--	--
Figure 11	0.93003	-7.00	+1.49965	-0.02762	0.15421	+0.43171	1.95909	-0.58954

Table 1
Extreme values of PLANCK's radiation-function and approximation according to the function ξ used without and with group delay correction

5. The WIEN displacement

The solution according to Figure 11 seems to fit to the best the observations. As we can see in figure 11, the curve oscillates around the nominal value near the upper cut-off-frequency, a behaviour, as we even know from technical minimum-phase low-pass filters (overshoot). Usually it is being suppressed by an attenuator and there is the parametric damping. Aside from that the level at the third null is already with -50dB , the rest disappears in noise.

Let's suppose, that the $_{-0.5}^{+1.5}\text{dB}$ are „healed up“ during the many billion years or have been „ironed out“ by other influences not considered here – at the end, we must carry out, as promised, a WIEN-displacement. Evidently the WIEN displacement law applies then. Most publications do not explain why it is called *displacement* law. Usually a graphic of nested curves for the wavelength λ is shown in a linear presentation. It should also be noted that the usual formula $\lambda=c/v$ cannot be used for the conversion $\omega_{\text{max}} \rightarrow \lambda_{\text{max}}$ for thermal spectra. The reason is the different radiation distribution. According to [10] applies $\lambda_{\text{max}}=0.6c/v_{\text{max}}$.

The name can only be properly understood in double logarithmic representation, e.g. in dB. Then you can see that the curves are really down-*shifted* along the left slope as temperature/frequency decreases (Figure 14). This can be achieved in a graphics program by moving the top right corner of the curve to the bottom left while holding down the Shift key. This results in a simultaneous reduction in frequency and amplitude. However, the

prerequisite is that the aspect ratio is equal to 1. Then the factor \tilde{x} describes exactly the distance between the peak value and the edge.

In principle, an explicit peak value is assigned to each peak frequency, including to the integral of the intensity over the entire frequency range, i.e. to the POYNTING vector \bar{S}_k . Before calculating the value \bar{S}_{kU} , we first determine \bar{S}_{k1} by extrapolating \bar{S}_{k0} . The values of Q_0 , ω_1 and T_k are known or can be calculated exactly. However, one peculiarity of the CMBR should be noted:



The cosmological background radiation CMBR is subject to the parametric damping, but not to the geometric damping.

The reason is that the entire universe is permeated by the radiation affecting the observer from all sides (state of equilibrium). We calculate the value \bar{S}_{kU} using the STEFAN-BOLTZMANN radiation law (409).

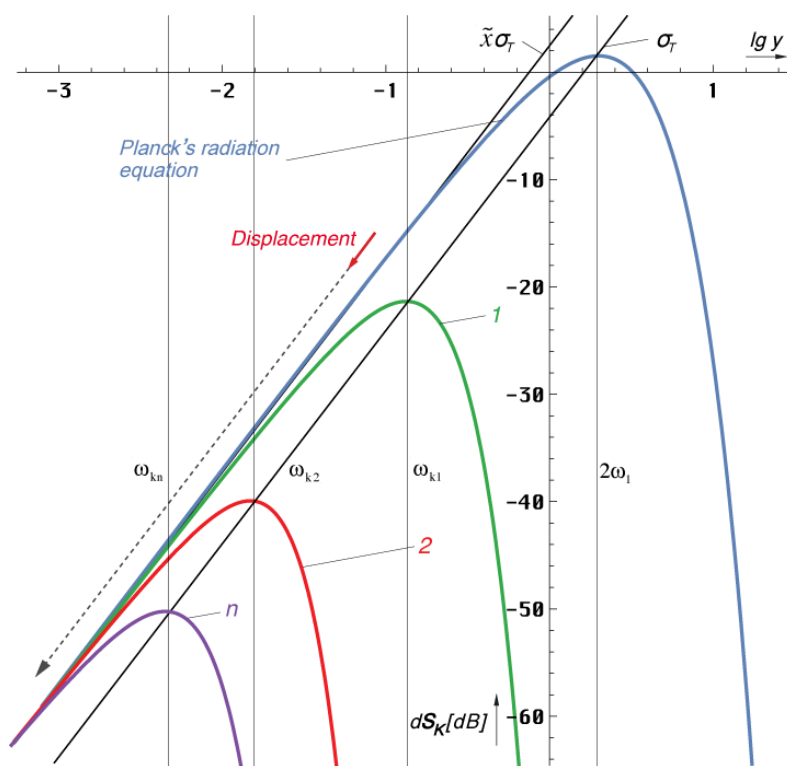


Figure 14
The WIEN displacement law
schematic presentation

However, this requires an exact determination of T_k . Of course we could use the COBE value for it, but we want to set up an accurate relation to Q_0 indeed. Therefore, at first, we will deal with T_k in the next section. All relevant frequencies are listed in Table 2, the values for $H_0 > 70$ are for information only.

Emission frequency ($H_0=68.6$)	ω_U	$3.09408 \cdot 10^{104} \text{ s}^{-1}$	f_e	$4.92438 \cdot 10^{103} \text{ Hz}$
Immission frequency ($H_0=68.6$)	ω_S	$6.85874 \cdot 10^{103} \text{ s}^{-1}$	f_s	$1.09160 \cdot 10^{103} \text{ Hz}$
CMBR-frequency ($H_0=75.9$)	ω_k	$1.12584 \cdot 10^{12} \text{ s}^{-1}$	f_k	179.18259 GHz
CMBR-frequency ($H_0=72.0$)	ω_k	$1.09639 \cdot 10^{12} \text{ s}^{-1}$	f_k	174.49511 GHz
CMBR-frequency ⁽⁶²⁾ ($H_0=68.6$)	ω_k	$1.00673 \cdot 10^{12} \text{ s}^{-1}$	f_k	160.22630 GHz
CMBR-frequency (COBE)	ω_k	$1.00675 \cdot 10^{12} \text{ s}^{-1}$	f_k	$160.23 \pm 0.1 \text{ GHz}$

Table 2
Frequencies of the cosmologic
background radiation

6. The temperature of the CMBR

With the help of the expressions given in [7] Section 4.6.4.2.5., we are able to calculate the temperature of the CMBR to compare it with the COBE-measuring. Indeed, it is hard to believe, that we can actually calculate back until a point of time before the phase jump at $Q=1$. But the contemplations conducted in [6] turned out, that both, photons – these behaved like neutrinos in the beginning – and electrons and protons, had had different properties shortly after BB, banish the usual notions of this period to the realm of imagination.

Albeit with a different value for H_0 ($71.9845 \text{ km s}^{-1} \text{ Mpc}^{-1}$), I succeeded in [1], to calculate a CMBR-temperature of 2.79146 K with the model. This was close to the $2.72548 \text{ K} \pm 0.00057 \text{ K}$ ($\pm 2.09137 \cdot 10^{-4}$), determined by the COBE-satellite. What works in one direction, naturally also works in the other direction. So the 2.72548 K of COBE using the values from [1] match an H_0 in the amount of $68.6072 \text{ km s}^{-1} \text{ Mpc}^{-1}$. Indeed, that's less than I calculated. Now, based on the electron, I determined, a new H_0 with an amount of $68.6241 \text{ km s}^{-1} \text{ Mpc}^{-1}$ in this work. And I was not a little surprised, that it was extremely close to the COBE-value. So I assume, that the new value must be more accurate, than the one calculated in [1]. Now to the calculation.

Whereas the temperature of the metric wave field is equal to zero (see below), it's not the case with the CMBR. Since it's about almost black radiation ($\varepsilon_v = 0.9428 = \frac{2}{3}\sqrt{2}$), we are able to calculate the *black temperature* indeed, but we want to work-on with the *grey temperature*. By transposing the WIEN displacement rule with the energetic redshift $z_{22} = 12 \varepsilon_v Q_0^{5/2}$ of (4) we obtain for $\omega_U = 2\omega_1$:

$$T_k = \frac{\hbar\omega_k}{\tilde{x}k} = \frac{\varepsilon_v}{\tilde{x}} \frac{\hbar_1\omega_1}{6k} Q_0^{-5/2} = 0.055693 \frac{\hbar_1\omega_1}{k} Q_0^{-5/2} \quad \tilde{x} = \begin{cases} 2.821439372 & \text{Exactly} \\ 2\sqrt{2} & \text{Approx.} \end{cases} \quad (57)$$

$$T_k = \frac{\hbar\omega_k}{\tilde{x}k} \approx \frac{1}{3} \frac{\hbar_1\omega_1}{6k} Q_0^{-5/2} = \frac{\hbar_1\omega_1}{18k} Q_0^{-5/2} \quad \varepsilon_v = \frac{\tilde{x}}{3} = 0.94048 \quad \text{Exactly} \quad (58)$$

That's the temperature of the cosmologic background radiation in consideration of the frequency response. The temporal course is shown in Figure 15 and 16. There are similarities to the energy density. The presentation of the spatial dependency should be omitted here.

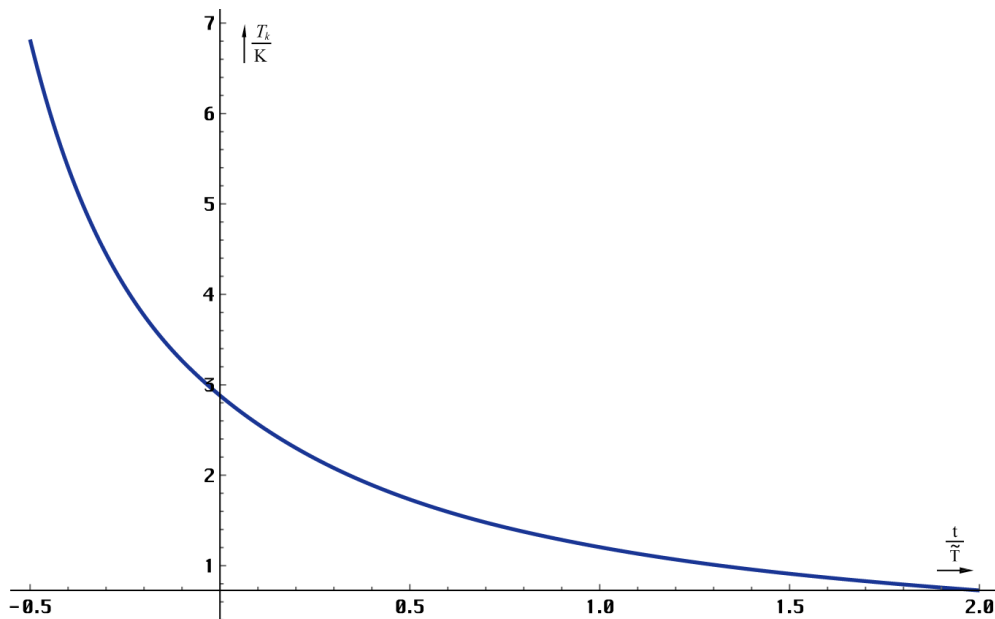


Figure 15
Temporal dependence of the radiation-temperature of the CMBR (linearly)

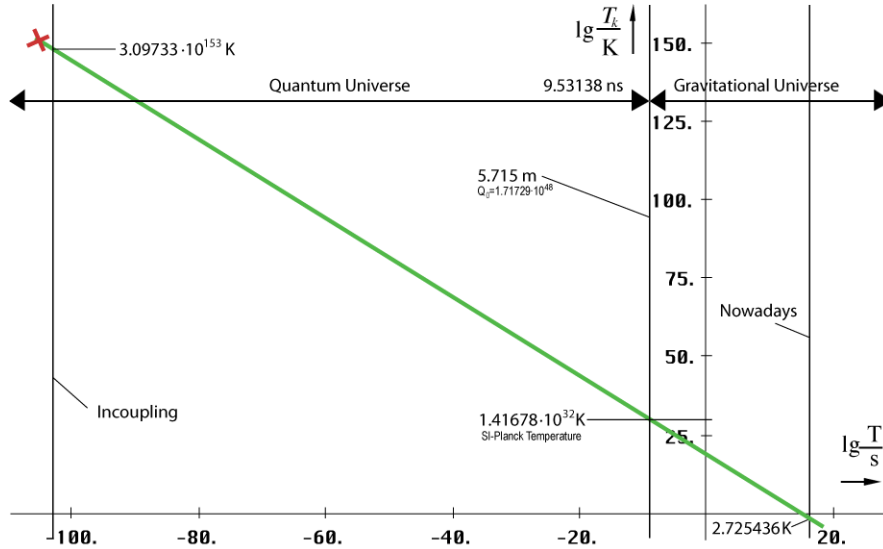


Figure 16
Temporal dependence of the radiation-temperature of the CMBR considered from the point of time of input coupling on

I already offered expression (58) as an approximation in [1], since the value $\tilde{x} = 3 + \ln(-3e^{-3})$ is only 0.25% below $2\sqrt{2}$, see also Section 3. With it, we get an extremely simple expression, which corresponds to a value $\varepsilon_v = \tilde{x}/3$. That would be $4 \times$ the 3 in one expression and the subspace slightly greyer, as thought. Since we want to know exactly, we will verify even this approach.

$$T_k = 1.002476662335245 \frac{\hbar_1 \omega_1}{18k} Q_0^{-\frac{5}{2}} \quad \varepsilon_v = \frac{2}{3} \sqrt{2} \quad (59)$$

$$T_k = 0.997209201884998 \frac{\hbar_1 \omega_1}{18k} Q_0^{-\frac{5}{2}} \quad \varepsilon_v = \delta \quad (60)$$

$$T_k = 1.000016126070630 \frac{\hbar_1 \omega_1}{18k} Q_0^{-\frac{5}{2}} \quad \varepsilon_v = 1.002814779667422 \quad (61)$$

The third, artificially created case for a “wonder” turns out the 2.72548K exactly. Table 3 shows all possible solutions once again including the accuracy limits of the COBE data.

Value	Q_0	H_0	H_0	CMBR Temperature	Absolute Difference	Relative Deviation
	[1]	[s ⁻¹]	[kms ⁻¹ Mpc ⁻¹]			
(890) [1]	$7.9518 \cdot 10^{60}$	$2.3328 \cdot 10^{-18}$	71.9843	2.791460	+0.06598	+2.42086
(59)	$8.3405 \cdot 10^{60}$	$2.2239 \cdot 10^{-18}$	68.6241	2.732186	+0.00671	+0.24605
(COBE) ₊	$8.3397 \cdot 10^{60}$	$2.2243 \cdot 10^{-18}$	68.6365	2.726050	+0.00057	+0.02091
(COBE) ₀	$8.3404 \cdot 10^{60}$	$2.2239 \cdot 10^{-18}$	68.6250	2.725480	±0.00000	±0.00000
(61)	$8.3405 \cdot 10^{60}$	$2.2239 \cdot 10^{-18}$	68.6241	2.725480	±0.00000	±0.00000
(62)	$8.3405 \cdot 10^{60}$	$2.2239 \cdot 10^{-18}$	68.6241	2.725436	-4.4 × 10 ⁻⁵	-0.00161
(COBE) ₋	$8.3411 \cdot 10^{60}$	$2.2236 \cdot 10^{-18}$	68.6135	2.724910	-0.00057	-0.02091
(60)	$8.3405 \cdot 10^{60}$	$2.2239 \cdot 10^{-18}$	68.6241	2.717830	-0.00765	-0.28069

Table 3
Calculated and measured CMBR-temperature in comparison with the values of the HUBBLE-parameter

The Q_0 - and H_0 -values for the COBE-satellite have been determined with the help of (58). The upper and the lower limits of the COBE-values are yellow highlighted. As we can see, the approximation (58) is very good. The value from [1] is much too high and (59) is outside the measuring precision of COBE. Expression (62) is out of question, since its value is below the measured one. Moreover it's not related to the model. That also applies to (61). The approximation (58) in contrast, seems to hit the nail on the head. Whether that's true, further, more precise measurements will prove. Thus, we define:

$$T_k = \frac{\hbar\omega_0}{18k} Q_0^{-\frac{1}{2}} = \frac{\hbar_1\omega_1}{18k} Q_0^{-\frac{5}{2}} = 2.725436049K \quad \Delta = -1.61258 \cdot 10^{-5} \quad (62)$$

The calculated value is within the accuracy limits of the value $2.72548K \pm 0.00057K$ measured by the COBE-satellite and is reference frame dependent ($\sim Q_0^{5/2}$). For the choose of the correct relation to the calculation of T_K I leave the reader room for his own interpretations. In addition, we want to calculate the corresponding frequencies for the technicians too. With the help of WIEN's displacement rule and (62) we get the following relations:

$$\omega_{\max} = \frac{1}{18} \tilde{x}\omega_1 Q_0^{-\frac{3}{2}} = 1.0067316 \cdot 10^{12} s^{-1} \quad v_{\max} = \frac{1}{36\pi} \tilde{x}\omega_1 Q_0^{-\frac{3}{2}} = 160.2263 \text{ GHz} \quad (63)$$

The factor σ of the STEFAN-BOLTZMANN radiation rule $\bar{S}_k = \sigma T^4 \mathbf{e}_s$ is also a function of Q_0 , see (89) in the next section for details. In [11] also the existence of a background field with neutrinos is postulated, which is said to have a temperature of approx. 1.9 K. Dividing T_k by $\sqrt{2}$ a value of 1.92717K turns out, which fits well the idea underlying this model that neutrinos propagate rectangularly to photons.

I have to make one more comment at this point. In the context of the publications about the PLANCK-units always is noted a so-called PLANCK-temperature T_θ . It's defined in the following manner:

$$T_\theta = \frac{m_0 c^2}{k} = 1.416784487 \cdot 10^{32} K \quad (64)$$

According to this model it should actually equal the temperature of the metric wave field, to be correct even divided by 8π . But that's not the case. According to [11] this results from the GIBBS fundamental equation to:

$$T_\theta dS_0 = d(mc^2) - \omega dL \quad (65)$$

$$T_\theta dS_0 = d(m_0 c^2) - \hbar\omega_0 dL = 0 \quad T_\theta \equiv 0K \quad (66)$$

because of $\omega_0 \neq \text{const}$. That well fits the observations. Thus, the famous expression $mc^2 = \hbar\omega$ is nothing other than a special case of the GIBBS fundamental equation for $T_\theta = 0$ at the level of the metric wave field. It thermally speaking, does not make an appearance – otherwise we would have been vaporised long ago. For the case $L=0$ the temperature would be expression (64) divided by 8π . Thus, the correct PLANCK-temperature T_θ is equal to zero. But it's possible to specify an initial CMBR-temperature for $Q_0=1$. It amounts to $T_{KI} = T_K Q_0^{5/2}$ $T_{KI} = 5.4753571754114 \cdot 10^{152} K$. The temperature at the in-coupling-time $t_1/4$ we get by multiplication with $2^{5/2}$ but the curve shape is no longer black then. See the next section for details.

7. Energy and entropy of the CMBR

By this we mean at first the POYNTING vector \bar{S}_k , but also the energy density w_k over the entire frequency range. As said, the calculation is done with the help of the STEFAN-BOLTZMANN radiation law (409). We do not know the values $\bar{S}_{k0.5}$, \bar{S}_{k1} , $w_{k0.5}$ and w_{k1} shortly

after Big Bang, but we want to calculate them. However, the current value of the energy density is given in [12], amounting to $w_{k0}=4.17 \cdot 10^{-14} \text{ J/m}^3$. That corresponds to a number of 411 photons/cm³. With it we can first calculate \bar{S}_{k0} . We are only interested in the amount:

$$w_{k0} = 4.17 \cdot 10^{-14} \text{ Jm}^{-3} \quad \bar{S}_{k0} = cw_{k0} = 12.5013 \mu\text{Wm}^{-2} \text{ [71dBpWm}^{-2}] \quad (67)$$

Now we substitute T_k in (409 [7]) with (62) obtaining the following expression:

$$\bar{S}_k = \sigma T_k^4 = \frac{\pi^2 k^4 T_k^4}{60c^2 \hbar^3} = \frac{\pi^2 k^4 T_k^4}{60c^2 \hbar^3} Q_0^3 \quad T_k^4 = \frac{\hbar_1^4 \omega_1^4}{18^4 k^4} Q_0^{-10} \quad (68)$$

However, the expression on the left is only valid for a single MLE. However, we consider a cube with the edge length r_0 , which contains a total of 4 pcs. Therefore we need to multiply by 4 obtaining:

$$\bar{S}_k = \frac{4\pi^2}{6298560} \frac{\hbar_1 \omega_1^4}{c^2} Q_0^{-7} = \frac{\pi^2}{1574640} \frac{\hbar_1 \omega_1^2}{r_1^2} Q_0^{-7} \quad (69)$$

It is better to use $/Q_0^4/Q_0^3$ instead of $\times Q_0^{-7}$ in the calculation, otherwise an underflow of values may occur. Interestingly enough, the BOLTZMANN constant k cancels out. That means that it cannot be calculated from other values. Also, it is the only constant which contains the Kelvin. That means, it's really fundamental and can be fixedly defined as how it happened.

Now in principle, we could calculate the value \bar{S}_{k1} by setting Q_0 in (69) equal to one. However, the expression is not yet complete. As already noted, the CMBR is subject to the parametric attenuation. Regardless of the reference frame, the damping factor α is always equal to $-1/R$, at which point R varies. α affects both, E and H , so we need to multiply (69) by $e^{-2r/R}$. Since the CMBR has always covered the maximum time-like distance $r=R=2cT$, the expression simplifies to e^{-2} . We expand the fraction by e^2 :

$$\bar{S}_k = \frac{\pi^2 e^2}{1574640} \frac{\hbar_1 \omega_1^2}{r_1^2} e^{-2} Q_0^{-7} \approx \left(\frac{1}{21592} \frac{\hbar_1 \omega_1^2}{r_1^2} \right) e^{-2} Q_0^{-7} \quad [21591.9850214238] \quad (70)$$

Because of the imprecise value of (67), we can work with the approximation with a clear conscience ($\Delta=-6.94 \cdot 10^{-7}$). With the bracketed expression \bar{S}_{k1} is actually already defined, but we have to find out whether it is correct.

$$\bar{S}_{k1} = \frac{1}{21592} \frac{\hbar_1 \omega_1^2}{r_1^2} = 2.596200 \cdot 10^{422} \text{ Wm}^{-2} \quad [4344.14\text{dB pWm}^{-2}] \quad (71)$$

$$w_{kl} = \frac{1}{21592} \frac{\hbar_1 \omega_1}{r_1^3} = \frac{\bar{S}_{k1}}{c} = 8.65999 \cdot 10^{413} \text{ Jm}^{-3} \quad [8.85872 \cdot 10^{418} w_l \text{ metrics}] \quad (72)$$

For comparison, the energy density w_l of the metrics. Here S_1 must be divided by $c_M[1]$ and multiplied by 4. The value w_{kl} is orders of magnitude below w_l . Attention, both \bar{S}_{k1} and w_{kl} are the values the CMBR would have, if the curve and thus the distribution were the same as today. As can be seen in Figure 2, the dynamic frequency response at $Q_0=1$ is not yet ready with its work. There is no PLANCK-distribution, but curve 4. This is quite similar to the target function curve 6, but not completely. However, \bar{S}_{k1} and w_{kl} are very well suited as fixed reference points.

Now we can use (70) to calculate the actual values and compare them with the measured ones (67):

$$\bar{S}_{k0} = \frac{1}{159544} \frac{\hbar_1 \omega_1^2}{r_1^2} Q_0^{-7} = \bar{S}_{k1} e^{-2} Q_0^{-7} = 1.25145 \cdot 10^{-5} \text{ Wm}^{-2} \quad [12.5013 \mu\text{W}^{-2}] \quad (73)$$

$$w_{k0} = \frac{1}{159544} \frac{\hbar_1 \omega_1}{r_1^3} Q_0^{-7} = w_{kl} e^{-2} Q_0^{-7} = 4.1744 \cdot 10^{-14} \text{Jm}^{-3} \quad [4.17 \cdot 10^{-14} \text{Jm}^{-3}] \quad (74)$$

That results in the local density of the CMBR background ($r \leq 0,01R$):

$$\rho_{k0} = \frac{1}{159544} \frac{\hbar_1 \omega_1}{c^2 r_1^3} Q_0^{-7} = \frac{w_{k0}}{c^2} = 4.64465 \cdot 10^{-34} \text{kgdm}^{-3} \quad [4.64 \cdot 10^{-34} \text{kgdm}^{-3}] \quad (75)$$

The values in square brackets are those given in [12]. The deviation of $-1.06 \cdot 10^{-3}$ is less due to a calculation error than to the fact that the comparative values are only given with two decimal places. Rather, the calculated values are accurate and actually much more accurate: $w_{k0} = 4.174403405098 \cdot 10^{-14} \text{Jm}^{-3}$, but only under the assumption that the CMBR has not interacted with other matter losing energy in the process. Since the deviation is a maximum of 0.1%, it does not appear to be the case. Because the model can be used to calculate back to $Q_0 = 1/2$ exactly, we can confidently shelve the idea of the CMBR origin 379,000 years after Big Bang. Then any thermal radiation would only be a narrow spectral line.

However, since in-coupling did not take place at $Q_0 = 1$ but at $Q_0 = 1/2$, there are 4 additional values of interest: \bar{S}_{k05} , w_{k05} , \bar{S}_{kU} as well as w_{kU} . The first two are again the values immediately after in-coupling, assuming a PLANCK distribution. To the calculation we use (73) and (74) by setting $Q_0 = 1/2$, e^2 is already contained in \bar{S}_{k1} .

$$\bar{S}_{k05} = \frac{16}{2699} \frac{\hbar_1 \omega_1^2}{r_1^2} = 128 \bar{S}_{k1} = 3.32313 \cdot 10^{424} \text{Wm}^{-2} \quad [4365.21 \text{dB pWm}^{-2}] \quad (76)$$

$$w_{k05} = \frac{16}{2699} \frac{\hbar_1 \omega_1}{r_1^3} = 128 w_{kl} = 1.10848 \cdot 10^{416} \text{Jm}^{-3} \quad [8.85872 \cdot 10^{418} w_l \text{ metrics}] \quad (77)$$

In reality, the values are much larger, since the curve has not yet been clipped at this point of time still matching the shape of a resonant circuit with the Q-factor $1/2$. The later POYNTING vector S_k results from the area ratio of the PLANCK-curve (11) and of the source curve S_T (1). I determined this by numerical integration.

$$S_k = 0.5503 S_T \quad (78)$$

Thus, if we want to determine the real in-coupling values \bar{S}_{kU} and w_{kU} , we have to divide by this value. Then we get:

$$\bar{S}_{kU} = \frac{1}{92.83} \frac{\hbar_1 \omega_1^2}{r_1^2} = 232.6 \bar{S}_{k1} = 6.038 \cdot 10^{424} \text{Wm}^{-2} \quad [4367.81 \text{dB pWm}^{-2}] \quad (79)$$

$$w_{kU} = \frac{1}{92.83} \frac{\hbar_1 \omega_1}{r_1^3} = 232.6 w_{kl} = 2.014 \cdot 10^{416} \text{Jm}^{-3} \quad [8.85872 \cdot 10^{418} w_l \text{ metrics}] \quad (80)$$

I have reduced the accuracy here because the area method does not necessarily reflect the actual conditions. I don't want to go back before the point $t_1/4$ (aperiodic borderline case), since there was no real wave propagation before. However, it is possible to determine the total energy that was used to build the CMBR. For this we need the real world radius at time $t_1/4$ ($Q_0 = 1/2$). This means that the volume is known and the total energy W_U can be calculated. We have already determined the exact world radius with the help of (45) lhs plus expansion implemented as the function $BRQ1[Q]$ multiplied by $Q^{3/2}$. There all angular and speed ratios are taken into account:

$$R_U = \frac{3}{2} r_1 Q^{\frac{3}{2}} \int_0^Q \frac{dQ}{\rho_0} = Q^{3/2} BRQ1[Q] r_1 \quad (81)$$

$$R_U = Q^{3/2} BRQI[Q]r_1 \quad \begin{cases} R_U(0.5) = 0.598337r_1 = 1.15949 \cdot 10^{-96} \text{ m} \\ R_U(1) = 9.207100r_1 = 1.78419 \cdot 10^{-95} \text{ m} \end{cases} \quad (82)$$

The course of the exact world radius is shown in Figure 17/18:

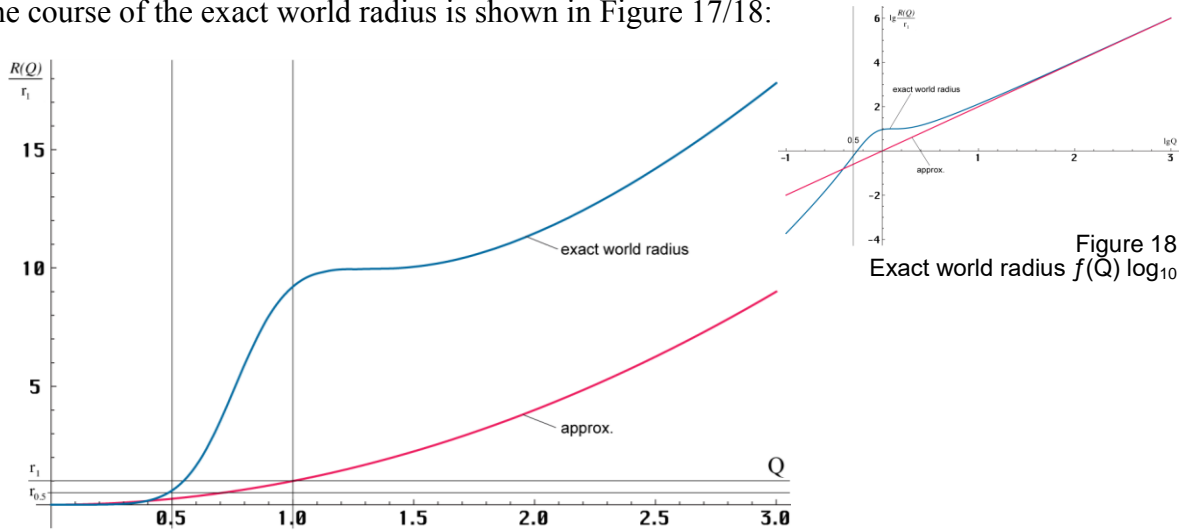


Figure 17
Exact world radius $f(Q)$ linear

Therefrom, the following volumina arise (spheric):

$$V_U = \frac{4}{3} \pi Q^{9/2} BRQI[Q]^3 r_1^3 \quad \begin{cases} V_U(0.5) = 0.897276r_1^3 = 6.52956 \cdot 10^{-288} \text{ m}^3 \\ V_U(1) = 3269.310r_1^3 = 2.37911 \cdot 10^{-284} \text{ m}^3 \end{cases} \quad (83)$$

Important for the calculation of W_{k05} is the answer to the question: How many line elements fit into the universe in actual fact. Regardless of whether we consider a sphere or a cube, because the factor $4/3\pi$ as well as r_1^3 cancel out, we get the following values with $r_0(Q) = Qr_1$:

$$N_U = Q^{3/2} BRQI[Q]^3 \quad \begin{cases} N_U(0.5) = 1.71367 \approx \sqrt{3} \\ N_U(1) = 780.491 \end{cases} \quad (84)$$

At the point of time $t_1/4$ ($Q_0 = 1/2$), the aperiodic borderline case, just one single line element fits into the universe, that's not a contradiction, while at $Q_0 = 1$ already 780 of them fit in. However, the number decreases to 180 at $Q_0 = 2,295$ in order to re-increase later approaching the function $N_U = Q_0^3$. Then, from 10^3 on the approximation applies, but not for long. For $R \gg 10^3 r_1$, r_0 decreases towards the edge and (362) from Section 4.6.1 of [7] applies.

$$N = \frac{2}{3} \pi \left(\frac{d}{\rho} \right)^3 = \frac{2}{3} \pi \left(\frac{\Lambda r_0}{r_0} \right)^3 = \frac{2}{3} \pi \Lambda^3 \quad (362 [7])$$

Λ is the constant wave count vector. This means that the line elements are arranged in a different packing at the beginning. At $Q_0 = 1$ there is a phase jump in the propagation function and thus a rearrangement towards f_c . The course of N_U exactly and approximation is shown in Figure 19.

Depending on your point of view, the universe begins with a negative entropy or with zero if we consider the state at $Q < 1/2$ as a feasible degree of freedom. Therefore, when calculating the immission energy W_{kU} we must decide whether we want to multiply the energy density w_{kU} by the volume of an MLE or that of the entire universe (83), and whether we want to choose a sphere or a cube. According to expression (84), a cube with the edge length r_1 also fits in, in its interior a line element with the radius $r = r_1/2$.

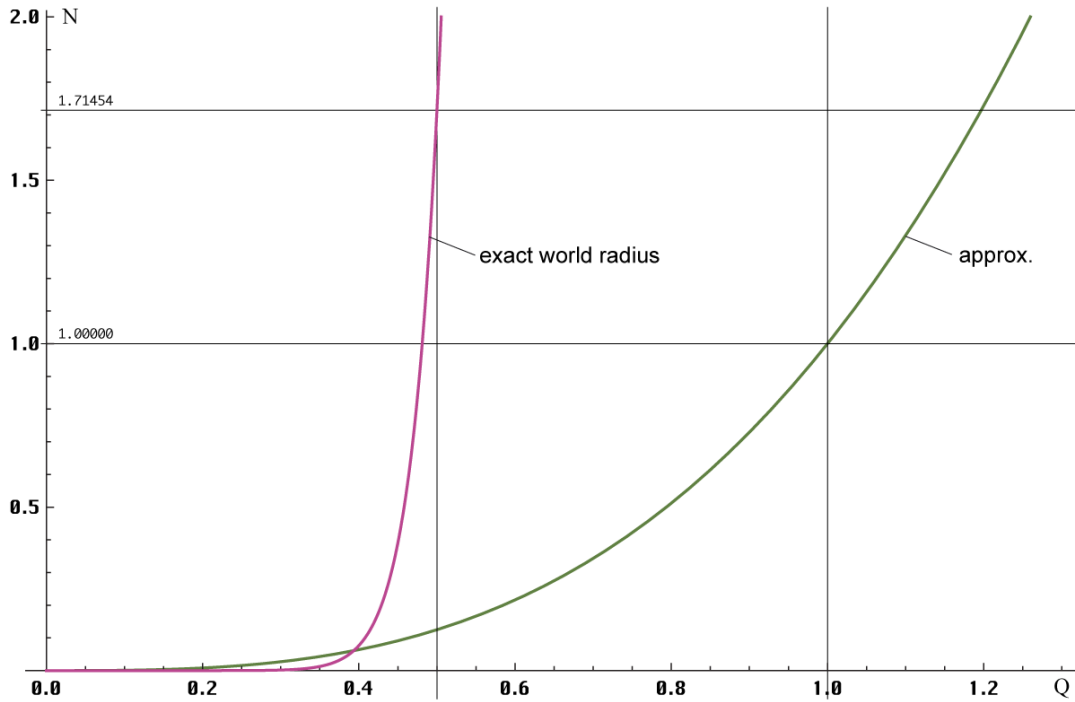


Figure 19
Maximum possible number of line elements N
in the universe at the beginning of expansion

Since we determined the other values using a cube, we choose the (inner) cube obtaining the volume $V_{\square} = 7.2771 \cdot 10^{-288} \text{ m}^3$. The outer sphere has a volume of $V_{\circ} = 1.97988 \cdot 10^{-287} \text{ m}^3$. For W_{kl} we choose the approximation because it's used as a fixed reference for larger values of Q_0 and also the cube with an edge length of r_1 . With it, the following values turn out:

$$\begin{aligned}
 W_{ku} &= 232.6 w_{kl} r_1^3 = \frac{1}{92.83} \hbar_1 \omega_1 = 1.46583 \cdot 10^{129} \text{ J} \\
 W_{kl} &\stackrel{\text{def}}{=} w_{kl} r_1^3 = \frac{1}{21592} \hbar_1 \omega_1 = 6.30195 \cdot 10^{126} \text{ J}
 \end{aligned} \tag{85}$$

This definition of W_{kl} has the advantage, that the value divided by $0.5503 \cdot 2^{-7}$ gives exactly the value of W_{ku} . With this we can now even calculate the costs of generating the CMBR. After the last price increase from my electricity provider, the kWh costs € 0.3560. That equals US\$ 0.39. Converted W_{ku} amounts to $4.07177 \cdot 10^{122} \text{ kWh}$, the costs to US\$ $1.588 \cdot 10^{122}$ including 19% VAT, a bargain compared to the costs of the metric wave field. This as a little fun by the way.

We now want to investigate whether we are able to derive an estimate of the current boson/fermion ratio from these values. It should also be possible to calculate the mean matter density, see Table 4. The photon number density at in-coupling looks very high but it applies per m^3 . If you multiply by the real volume r_1^3 , you get 0.01 only. Since in fact only integer n can occur, we should get used to round-up to the next integer (Ceiling[#]), then it'll be fine. Please find the calculation further down.

The value ρ_{k0} (75) agrees very well with that given in [12], even if the formula stated there is completely unsuitable for calculation, since essential components have been omitted as »usual«. The same applies to the photon number density. Here the conditions are even more complicated.

The value $411/\text{cm}^3$ specified there is plausible. I've been trying to find a formula that calculates this. With [12] you get a totally wrong result of 5 photons per K^3 . A unit of length does not appear there. Still best of all one fares with [11]. On p. 197 in the continuous text $n_\gamma = 0.37 \text{ bK}^{-1} T_\gamma^3$ is given.

Value	Poynting vector	dB	Energy density	Symb.	Definition	Number/m ³
Beginning	$6.0380 \cdot 10^{424} \text{Wm}^{-2}$	4367.81	$2.014 \cdot 10^{416} \text{Jm}^{-3}$	W_{kU}	Immission	$1.30 \cdot 10^{284}$
Target now	$1.25145 \cdot 10^{-5} \text{Wm}^{-2}$	70.9742	$4.1744 \cdot 10^{-14} \text{Jm}^{-3}$	W_{kO}	Bosons target	$4.245 \cdot 10^8$
Actual now	$1.25013 \cdot 10^{-5} \text{Wm}^{-2}$	70.9696	$4.17?? \cdot 10^{-14} \text{Jm}^{-3}$	n_γ	Bosons actual	$4.105 \cdot 10^8$
Density	Target now local ρ_{kO}	—	$4.645 \cdot 10^{-34} \text{g cm}^{-3}$	n_M	Fermions	45.81948
Density	Target now local ρ_{GO}	—	$7.410 \cdot 10^{-29} \text{g cm}^{-3}$	n_γ/n_M	Ratio	$8.958 \cdot 10^6$

Table 4
Field strength and energy density of the
cosmologic background radiation ($H_0=68.6$)

Here k is the BOLTZMANN constant and b should be the STEFAN-BOLTZMANN-constant σ , which of course is defined differently again, so that the text formula has to be adapted. Then, with the COBE value we get:

$$n_\gamma = 1.48 \frac{\sigma}{k \cdot c} T_{kO}^3 = 410.466 \text{ cm}^{-3} = 4.10466 \cdot 10^8 \text{ m}^{-3} \quad (86)$$

That's actually only 410 photons, but we always wanted to round up in future. So I tried to figure out how to get to 0.37 to increase accuracy and failed miserably. After studying various sources, I do not refer to erroneous publications, it has been shown that the factor amounts to $2\zeta(3)/\pi^2$. It results from the solution of an integral, $\zeta(x)$ is Riemann's zeta function. But I don't get a correct result with it. Rather it should be $4\zeta(3)/\pi=1.53$. There is probably a third, different definition of σ . We use the CODATA₂₀₁₈ definition. With it, we obtain the correct expression:

$$n_\gamma = 4\zeta(3) \frac{\sigma}{\pi k c} T_{kO}^3 = 424.473 \text{ cm}^{-3} = 4.24473 \cdot 10^8 \text{ m}^{-3} \quad (87)$$

But now, with the COBE value of T_k , it are not 411, but 425 photons. What that means I leave open here. It's possible that one solution applies to the frequency, the other to the wavelength. Since both T_{kO} (62) and σ (409 [7]) depend on the reference frame, it should be possible to describe the photon number density of the CMBR as a function of Q_0 and thus even of t . Expression (62) is already correct, still σ remains. It contains \hbar^{-3} . We define:

$$\sigma_1 = \frac{\pi^2 k^4}{60 \hbar^3 c^2} = \text{const} = 9.773258655978905 \cdot 10^{-191} \text{ Wm}^{-2} \text{ K}^4 \quad (88)$$

$$\sigma = \frac{\pi^2 k^4}{60 \hbar^3 c^2} = \sigma_1 Q_0^3 = 5.6703666738854964 \cdot 10^{-8} \text{ Wm}^{-2} \text{ K}^4 \quad (89)$$

This of course eliminates the fixation of σ , which passes over to σ_1 , just like with \hbar . Using (409 [7]) and (62) we get then for the photon number density:

$$n_\gamma = 1.48 \frac{\sigma_1 T_{kl}^3}{k \cdot c} Q_0^{-9/2} = \frac{r_1^{-3}}{23955.6} Q_0^{-9/2} \quad [\text{m}^{-3}] \quad (90)$$

Now we only used the photons of the cosmic background radiation to determine the photon number density. In reality, of course, there are also photons that have nothing to do with it, that originate from interaction processes or were created during the annihilation of matter and antimatter. A large part of the cosmic radiation spectrum comes e.g. from supernova explosions. So we have to correct the photon number slightly upwards. The graphical presentation follows further down together with the nucleon number density n_M in Figure 23. However, before we are able to determine n_M , we need to have a look at entropy again.

Since the letter S is already heavily overburden, we must exercise special caution here. We had already used S_b , S_0 and S_1 for the entropy of the metric wave field, and S_0 , S_1 and $\overline{S}_{k0/1/U}$ for the POYNTING vectors. Now we still need an expression for the specific entropy per nucleon.

In [11] the expression \overline{S}_γ is used for this. Since the letters U and M can also appear in this context, we use \underline{S}_γ instead. According to [11] »the specific entropy S_γ/M or – as a dimensionless quantity – its entropy per nucleon \underline{S}_γ measured in natural entropy units, $\underline{S}_\gamma \equiv m_a \times k^{-1} S_\gamma/M$... provides us with extraordinarily important information about the early days of the universe«. The third power is used there too, $M = \rho_G R^3$ is the total mass of the fermionic matter, m_a the nucleon mass, i.e. the atomic mass unit. We have to convert the formula given there for the calculation of \underline{S}_γ again:

$$\underline{S}_\gamma = \frac{16}{3} \frac{\sigma m_a}{kc\rho_G} T_k^3 = 2.4562 \cdot 10^{-21} \rho_G^{-1} \text{kgdm}^{-3} \quad (4.101 [11])$$

To determine the matter density ρ_G we need the rest mass M of the incoherent matter of the entire universe. For this purpose, counts in the starry sky and estimates were carried out in the past, or one relied on a world model. I would like to expressly refrain from the calculation according to [11], since it uses the standard model, which this model is guaranteed *not* based on. Actually, we only need one mass and which one is the most suitable for this purpose? The MACH-mass $M_1 = \mu_0 k_0 \hbar$ from Section 6.2.4.1. of [7]. This already represents the average relevant for the observer. It applies $M_1 = \rho_G R^3$. This gives us the current value for ρ_{G0} :

$$\rho_{G0} = M_1 R^{-3} = 7.41028 \cdot 10^{-29} \text{kgdm}^{-3} \quad (91)$$

The value of ρ_G is based on the cube and agrees reasonably with the value $\rho_G \approx 10^{-30} \text{g/cm}^3$ given in [11]. Other publications indicate values of $0.3 \dots 1.1 \cdot 10^{-30} \text{kg/dm}^3$ for the density. However, these are only estimates. The entropy per nucleon $\underline{S}_{\gamma 0}$ ($2.4 \cdot 10^{-9}$) differs significantly. The cause is the outdated value of H_0 in the amount of $55 \text{ km s}^{-1} \text{ Mpc}^{-1}$ and the standard model used there.

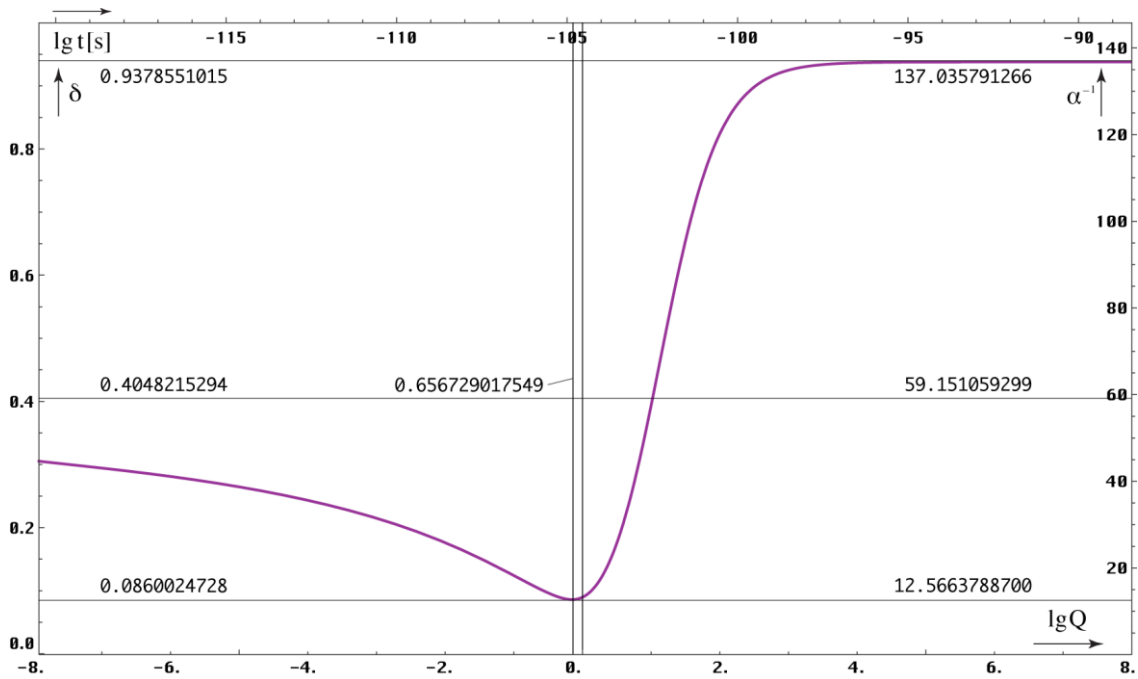


Figure 20
Correction factor δ and reciprocal of the fine-structure-constant α as a function of time after BB and of the phase angle Q

For $\underline{S}_{\gamma 0}$ we use (409 [7]) and (62) once more and we first replace m_a by m_e . Since the ratio m_p/m_e has been proven to be constant [13], the same applies to m_a/m_e and $\underline{S}_{\gamma 0}$ too. By rear-

ranging (806 [7]) with $M_1=9\pi^2\sqrt{2}\delta m_e Q_0^{4/3}$ we can now substitute m_e by M_1 and we get for the approximation:

$$\underline{S}_{\gamma_0} = \frac{16 \sigma m_a}{3 kc\rho_G} T_k^3 = \frac{16 \cdot 1822.8884862}{3 \cdot 60 \cdot 18^3 \cdot 9 \cdot \sqrt{2}} \delta^{-1} Q_0^{1/6} \approx \frac{1}{429.638496677} Q_0^{1/6} \quad (92)$$

The value of δ is defined by (806 [7]) as $\delta=4\pi/\alpha m_e/m_p=\text{const}$ for all generic cases and as variable functions $\text{deltaF}[Q]$ using $\text{alphaF}[Q]$ immediately after BB with $Q \leq 10^3$, that's an age of $T \leq 2.13 \cdot 10^{-97} \text{s}$ (Definition see Appendix).

In fact, all constants can be eliminated and only one constant factor and Q_0 remain. Here, the dependency on Q_0 is only considered for σ . To $R(Q)$ the approximation $R=Q_0^2 r_1$ applies and to m_a the linear approximation $1822.9 m'_e$ from Figure 15. If we want to use the exact functions, we need the function $\text{BRQ1}[Q]$ for the exact world radius, the function $\text{deltaF}[Q]$, and expression (806 [7]). Then, the exact expression reads:

$$\underline{S}_{\gamma_0} = \frac{1}{458.107543477} \text{BRQ1}[Q_0]^3 \text{deltaF}[Q_0]^{-1} Q_0^{-4/3} = 3.31458 \cdot 10^7 \quad (93)$$

All non-linearities in the world radius and the nucleon mass shortly after Big Bang are taken into account here. The results of (92) and (93) for Q_0 are identical since $Q_0 \gg 1$.

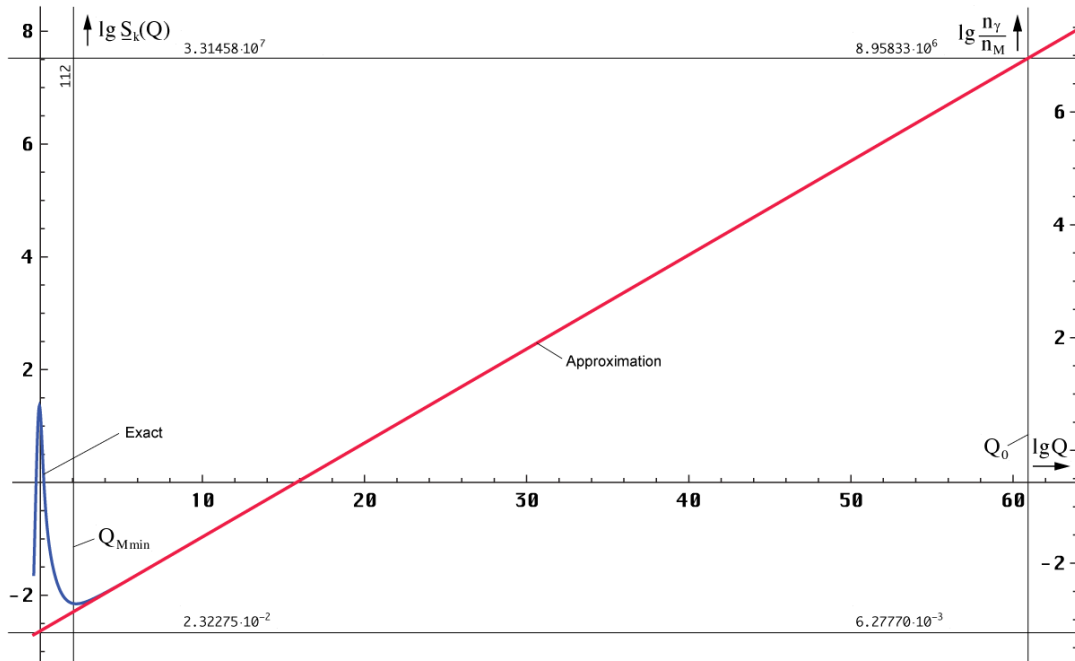


Figure 21
Entropy per nucleon and photon/nucleon-
ratio of the CMBR large scale

Now we can also calculate the nucleon number density n_M . According to [11] the quotient n_γ/n_M is proportional \underline{S}_γ . It applies:

$$\underline{S}_\gamma = 3.7 \frac{n_\gamma}{n_M} \quad \frac{n_\gamma}{n_M} = 8.95833 \cdot 10^6 \quad n_M = 45.8195 \text{ m}^{-3} \quad (4.102 [11])$$

$$n_M = \frac{r_1^{-3}}{14.133123} \text{BRQ1}[Q_0]^{-3} \text{deltaF}[Q_0] Q_0^{-19/6} \approx \frac{r_1^{-3}}{15.069623} Q_0^{-14/3} \quad (94)$$

Now we have determined the current values. Thus, we can calculate the course of \underline{S}_γ for larger and smaller values as a function of Q . It is shown in Figure 21 and 22.

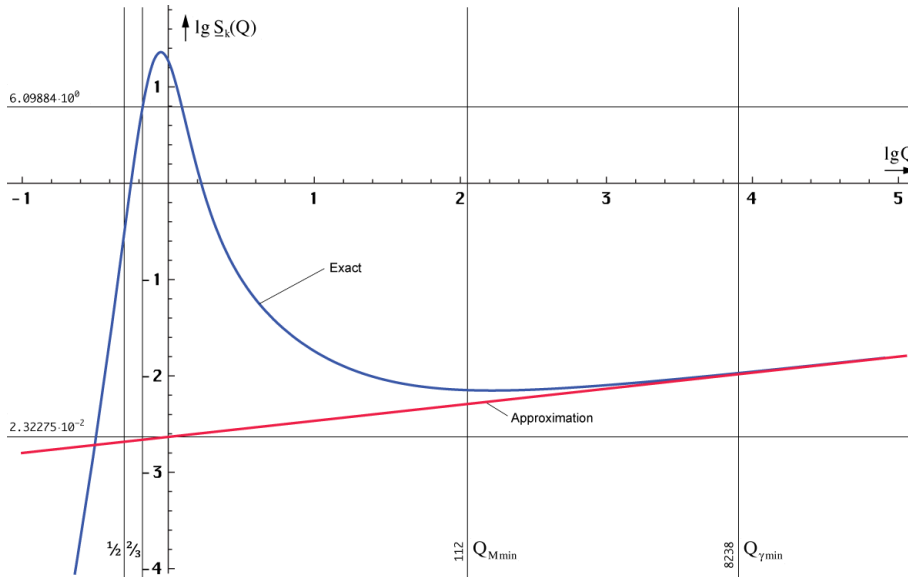


Figure 22
Entropy per nucleon of
the CMBR small scale

Now there is the well-known *initial entropy problem* with the standard model, i.e. it is assumed that the universe was in thermodynamic equilibrium at BB, a state of maximum entropy. However then, at the origin of the CMBR at 3000K the entropy must have been lower in order for it to increase over time, since a decrease without energy addition is physically forbidden. After the BB, however, there was no more energy supply. Therefore, most people blame it on the influence of gravity.

Now I had thought that this problem does not exist with my model, since the CMBR here is related to the point $Q = 1/2$, i.e. much earlier. If you take a closer look at Figure 22, however, you can see that there is also a section where the entropy decreases. The question is now, is there such a problem with my model too? The answer is: No. In reality, it is a statistical problem.

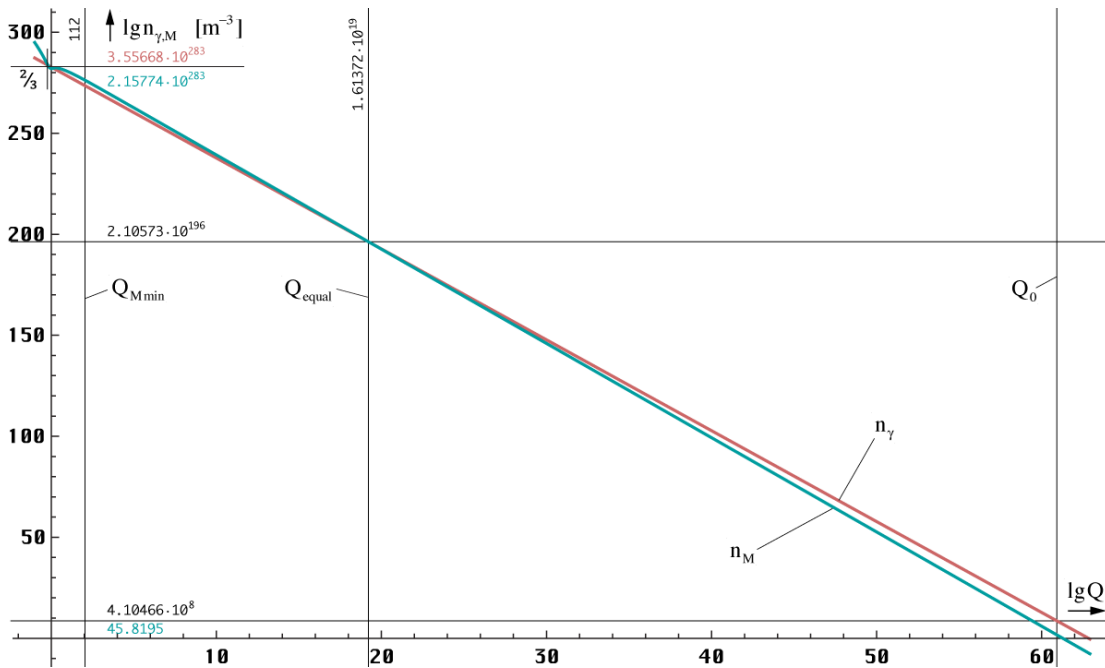


Figure 23
CMBR-photon-number- in comparison
to the nucleon-number-density per m^3

Even if the mass, photon- and nucleon-number density assumes impressively high values shortly after BB, the number of particles involved is very small, since the world radius is

extremely small at this time. Since entropy is a statistical variable, but statistics requires a minimum number of possible degrees of freedom (particles) in order to generate relevant results, the results are not relevant if this number is not reached, nor violations of physical principles. I assumed the minimum value to be 32 and marked it in picture 80. There are two different values, one for nucleons ($Q=112$), the other for photons ($Q=8238$), after that, i.e. from $2.13 \cdot 10^{-97}$ s after BB on, there were no more violations and therefore no problem. Before that, quantum effects predominated, which defy any statistics.

Therefrom follows that it is generally sufficient to use the approximation formulas. Figure 23 shows the photon- (90) and the exact nucleon-number density (94) as a function of Q . As you can see, there were initially more nucleons than photons. The parity was reached at the point of time $8.42 \cdot 10^{-67}$ s after BB.

Today there are more photons than nucleons. So we live in a largely radiation-dominated universe. How do we get the time data? Very easy, it applies $t=Q^2 t_1$. In the logarithmic presentation the x-axis has to be multiplied by 2 only. In contrast to the impressively high values, Figure 24 shows the actual number of CMBR photons and nucleons in the entire universe.

So today there are $1.19674 \cdot 10^{80}$ nucleons in the universe. This value corresponds almost exactly to the square of the value C (1038 [7]) described by EDDINGTON, which he already assumed to correspond to the total number of nucleons in the universe, see Section 7.5.1. of [7]. So it seems that the number of photons and nucleons is closely linked to the reference frame and thus to the age of the universe. So the universe *requires* the presence of a certain number of particles at a certain point of time. This is ensured by a certain number of particles decaying into several others, as well as by virtual pairing/annihilation processes.

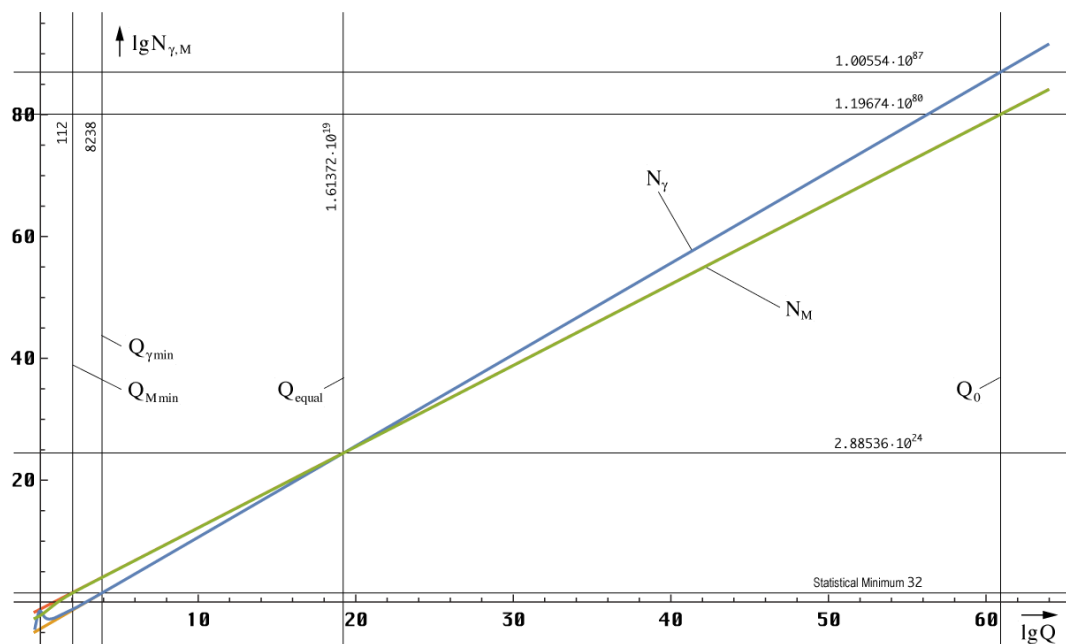


Figure 24
Real number of CMBR-photons
and nucleons in the whole universe

These processes are triggered by entropy. For example, you can assign a certain entropy to an isotope. The larger the value, the shorter the half-life. Because of (708 [7]) entropy also depends on the velocity. Thus atoms at high velocities not only decay more slowly because time passes more slowly, but also because the entropy is lower. Both statements describe the same fact and are equivalent.

$$Q_0 = \tilde{Q}_0 \left(\left(1 + \frac{t}{\tilde{T}} \right)^{\frac{1}{2}} - \left(\frac{2r}{\tilde{R}} \right)^{\frac{2}{3}} \right) \left(1 - \frac{v^2}{c^2} \right)^{\frac{1}{3}} \quad (708 [7])$$

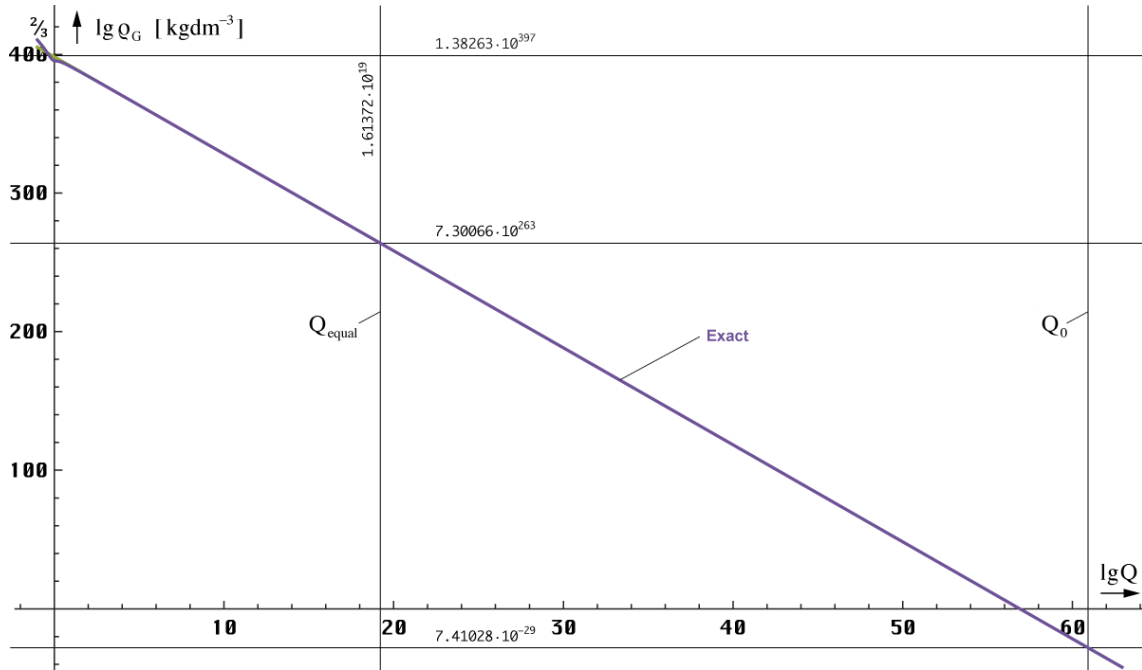


Figure 25
Dependence of the incoherent matter density considered from the time of in-coupling on

The only thing missing is the density of the incoherent matter ρ_G , which is also a function of time and space. The course is shown in Figure 25 and 26. The density is defined as follows:

$$\rho_G = \frac{M_2}{r_1^3} BRQ1[Q_0]^{-3} Q_0^{-11/2} \approx \frac{M_2}{r_1^3} Q_0^{-7} \tag{95}$$

In contrast to (91), the value M_2 (fixed) is used here instead of M_1 , since M_1 also depends on the reference frame and thus on time. It applies $M_1 = M_2/Q_0$.

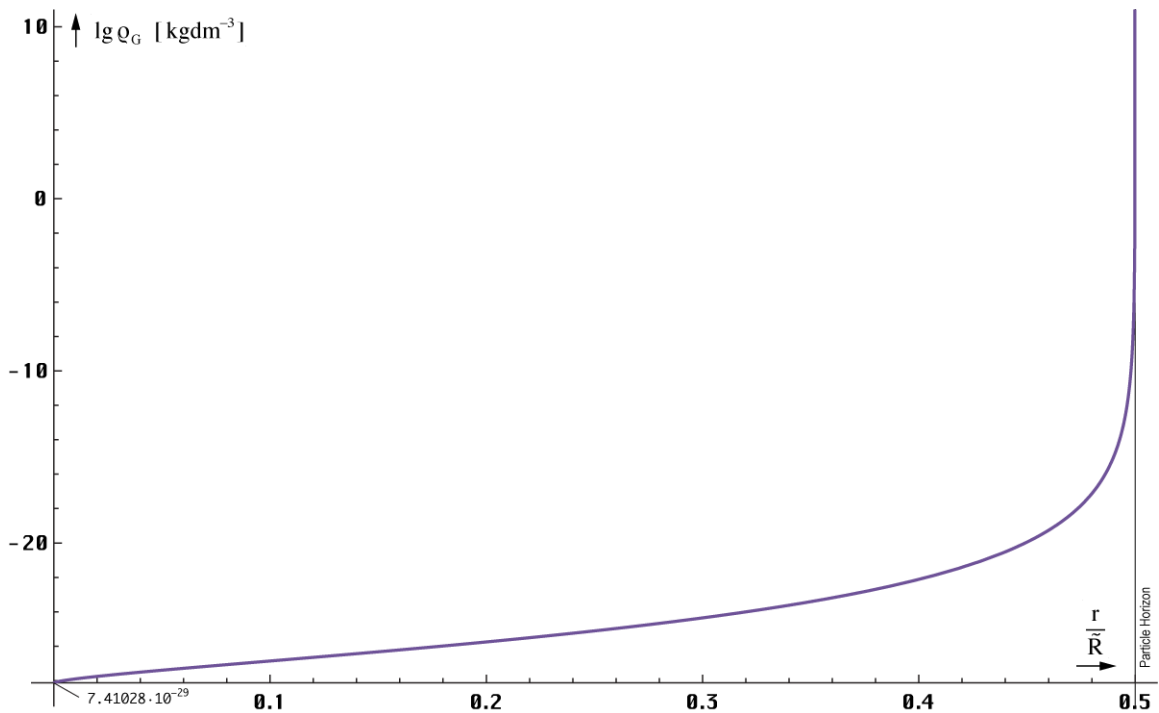


Figure 26
Spatial dependence of the incoherent matter density to the point of time T (nowadays)

Since all previous values are dependent on Q_0 , one can also show the dependence on other quantities using (708 [7]). Figure 26 shows the dependency on the distance r using the example of incoherent matter density. The further away we observe, the older the condition we observe. However, it is relevant for us because even delayed effects are effects.

Thus, most of the mass is located at the edge for each observer, evenly distributed over the particle horizon (repulsion!), so that the forces cancel each other. However, when accelerating, one leaves the center and must exert a force $F=m \cdot a$. With it, the MACH mass M_1 is the cause of the inertial mass, exactly as postulated by MACH. For antimatter a different equivalence principle applies $m_i = -m_g$, so that it is attracted by the particle horizon.

8. Summary

In the course of this article, according to the model in [7], we succeeded in approximating the envelope-curve of PLANCK's radiation law as a function of a dynamic frequency response under application of a phase- and group-delay-correction with a residual deviation of ${}_{-0,5}^{+1,5}$ dB. Furthermore it was shown, that the temperature calculated in [1] is in the proximity of the value measured by the COBE-satellite. With the help of the updated values of H_0 and Q_0 , determined in [6] and [7] a more recent CMBR-temperature could be calculated, which well fits the accuracy limits of the radiation temperature, measured by the COBE/WMAP-satellite. The results of this work point out, that origin and progression of the CMBR have elapsed in a totally different manner than generally assumed. Because photons behaved like neutrinos at that time they did not interact with other matter shortly after BB. Thus, the model can be used to calculate back to $Q_0 = 1/2$ exactly and we can confidently shelve the idea of the CMBR origin 379,000 years after Big Bang. Otherwise it would be a discrete, very narrow spectral-line.

9. Affidavit

Herewith, I declare that I created this work off my own bat having used no other aids as stated. With publications of this work in German language, a transcription according to the rules of the new orthography (1999 and later) is not allowed. This work and all translations of it must not be gendered under any circumstances.

10. Notes on the Appendix

With the help of the model in [7], it was possible to calculate a series of natural constants associated with the electron, the proton and the ${}^1\text{H}$ atom via their relationship to the reference system Q_0 and this exactly. The maximum deviation of $\pm 1.0 \cdot 10^{-9}$ for the THOMSON cross section σ_e corresponds to the standard deviation of the numerical value given in Table 5.

In fact, most values are not true constants. At the same time, the value of H_0 could be specified more precisely, as well as the value of κ_0 , the specific conductivity of the vacuum, on which this model is based. Since we have uncovered the relations between the individual fundamental constants, it is appropriate to develop a program with which these are recalculated on the spot each time according to the reference system and to use it instead of a list of values determined independently of one another in different laboratories. With regard to the list, this would also have the advantage that the errors would not add up.

The model is based on the fundamentals of subspace, which are fixed values and independent of the frame of reference. At this point it suffices to define only five genuine constants (μ_0 , c , κ_0 , \hbar_1 and k) as fixed basic values plus a so-called *magic value*, here m_e , in order to identify the reference frame Q_0 .

The formulae and definitions used in this work, and the programs to the calculation of the values in column 3 of Table 5 as well as for rendering the graphics are shown in the Appendix. It's about the source code for *Mathematica*. If you dispose of a pdf-version of this article, you are able to convert the data into a text file (UTF8), which can be opened directly. The data is presented as a single cell then. However, it is not advantageous to evaluate the entire source code in one single cell. To split, use the Cell/Divide Cell function (Ctrl/Shift/d). However, with this procedure there may be problems with special characters, not correctly transferred (e.g. ϵ , ϵ) or even lead to the conversion being aborted.

It is more advantageous to copy and paste data page by page into the text file via clipboard. However, then each line is present as a separate cell. With the command Cell/Merge (Ctrl/Shift/m) the cells belonging together can be merged, ideally in blocks between the headings. Expressions within (*...*) are comments for better understanding.

If you want to calculate only some values and not the graphics, you can delete the notebook below the point "End of Metric System Definition". Then, the values shown in column 3 are available for own calculations. The program to calculate the whole table can be found in [7].

Symbol	Variable	Calculated (CA)	Source	CODATA ₂₀₁₈ (CD) © COBE Data	±Accuracy	Δy (CA/CD-1)	Unit
c	c	2.99792458 · 10 ⁸	S	2.99792458 · 10 ⁸	defined	defined	m s ⁻¹
ϵ_0	ep0	8.854187817620390 · 10 ⁻¹²	S	8.854187817620390 · 10 ⁻¹²	defined	defined	As V ⁻¹ m ⁻¹
K_0	ka0	1.369777663190222 · 10 ⁹³	S	n.a.	n.a.	defined	A V ⁻¹ m ⁻¹
μ_0	my0	1.256637061435917 · 10 ⁻⁶	S	1.256637061435917 · 10 ⁻⁶	exactly	exactly	Vs A ⁻¹ m ⁻¹
k	k	1.3806485279 · 10 ⁻²³	S	1.380649 · 10 ⁻²³	statistic	+3.41941 · 10 ⁻⁷	J K ⁻¹
\hbar_1	hb1	8.795625796565460 · 10 ²⁶	S	n.a.	n.a.	defined	J s
\hbar	hb0	1.054571817000010 · 10 ⁻³⁴	C	1.054571817 · 10 ⁻³⁴	defined	+8.88178 · 10 ⁻¹⁵	J s
Q_0	Q0	8.340471132242850 · 10 ⁶⁰	C	8.3415 · 10 ⁶⁰ ©	3.3742 · 10 ⁻²	-1.23343 · 10 ⁻⁴	1
Z_0	Z0	376.7303134617700	F	376.73031366857	1.5 · 10 ⁻¹⁰	-5.48932 · 10 ⁻¹⁰	Ω
G	G0	6.674301499999827 · 10 ⁻¹¹	C	6.674301499999999 · 10 ⁻¹¹	2.2 · 10 ⁻⁵	-5.48932 · 10 ⁻¹⁰	m ³ kg ⁻¹ s ⁻²
G_1	G1	9.594550966819210 · 10 ⁻¹³³	C	n.a.	n.a.	unusual	m ³ kg ⁻¹ s ⁻²
G_2	G2	1.150360790738584 · 10 ⁻¹⁹³	F	n.a.	n.a.	unusual	m ³ kg ⁻¹ s ⁻²
M_2	M2	1.514002834704114 · 10 ¹¹⁴	F	n.a.	n.a.	unusual	kg
M_1	M1	1.815248576128075 · 10 ⁵³	C	n.a.	n.a.	unusual	kg
m_p	mp	1.6726219236951 · 10 ⁻²⁷	C	1.6726219236951 · 10 ⁻²⁷	1.1 · 10 ⁻⁵	-2.22045 · 10 ⁻¹⁶	kg
m_e	me	9.109383701528 · 10 ⁻³¹	M	9.109383701528 · 10 ⁻³¹	3.0 · 10 ⁻¹⁰	magic ±0	kg
m_0	m0	2.176434097482374 · 10 ⁻⁸	C	2.176434097482336 · 10 ⁻⁸	calculated	+1.70974 · 10 ⁻¹⁴	kg
M_H	MH	2.609485798792167 · 10 ⁻⁶⁹	C	n.a.	n.a.	unusual	kg
m_e/m_p	mep	5.446170214846793 · 10 ⁻⁴	F	5.4461702148733 · 10 ⁻⁴	6.0 · 10 ⁻¹¹	-4.867 · 10 ⁻¹²	1
T_p	Tp	0.000000000000000	C	1.416784486973588 · 10 ³²	calculated	MOOP	K
T_{k1}	Tk1	5.475357175411492 · 10 ¹⁵²	C	n.a.	n.a.	unusual	K
T_k	Tk0	2.725436049425770	C	2.72548 ©	4.3951 · 10 ⁻⁵	-1.61258 · 10 ⁻⁵	K
r_1	r1	1.937846411698606 · 10 ⁻⁹⁶	F	n.a.	n.a.	unusual	m
r_0	r0	1.616255205549261 · 10 ⁻³⁵	C	1.616255205549274 · 10 ⁻³⁵	calculated	-8.21565 · 10 ⁻¹⁵	m
r_e	re	2.817940324662071 · 10 ⁻¹⁵	C	2.817940326213 · 10 ⁻¹⁵	4.5 · 10 ⁻¹⁰	-5.50377 · 10 ⁻¹⁰	m
λ_C	λ barC	3.861592677230890 · 10 ⁻¹³	C	3.861592679612 · 10 ⁻¹³	3.0 · 10 ⁻¹⁰	-6.16614 · 10 ⁻¹⁰	m
λ_C	Λ C	2.426310237188940 · 10 ⁻¹²	C	2.4263102386773 · 10 ⁻¹²	3.0 · 10 ⁻¹⁰	-6.13425 · 10 ⁻¹⁰	m
a_0	a0	5.291772105440689 · 10 ⁻¹¹	C	5.291772109038 · 10 ⁻¹¹	1.5 · 10 ⁻¹⁰	-6.79793 · 10 ⁻¹⁰	m
R	R	1.348032988422084 · 10 ²⁶	C	n.a.	at issue	at issue	
R	RR	4.368617335409830	C	n.a.	at issue	at issue	Gpc
t_1	2 t1	6.463959849512312 · 10 ⁻¹⁰⁵	F	n.a.	n.a.	unusual	s
t_0	2 t0	5.391247052483426 · 10 ⁻⁴⁴	C	5.391247052483470 · 10 ⁻⁴⁴	calculated	-8.43769 · 10 ⁻¹⁵	s
T	2 T	4.496554040802734 · 10 ¹⁷	C	4.497663485280829 · 10 ¹⁷	1.1385 · 10 ⁻³	-2.46671 · 10 ⁻⁴	s
T	2 T	1.424902426903056 · 10 ¹⁰	C	1.425253996152531 · 10 ¹⁰	1.1385 · 10 ⁻³	-2.46671 · 10 ⁻⁴	a
R_∞	R_∞	1.097373157632934 · 10 ⁷	C	1.097373156816021 · 10 ⁷	1.9 · 10 ⁻¹²	+7.44426 · 10 ⁻¹⁰	m ⁻¹
ω_1	Om1	1.547039312249824 · 10 ¹⁰⁴	F	n.a.	n.a.	unusual	s ⁻¹
ω_0	Om0	1.854858421929227 · 10 ⁴³	C	1.854858421929212 · 10 ⁴³	calculated	+8.65974 · 10 ⁻¹⁵	s ⁻¹
ω_{R_∞}	OmR ∞	2.067068668297942 · 10 ¹⁶	C	2.067068666759112 · 10 ¹⁶	1.9 · 10 ⁻¹²	+7.44451 · 10 ⁻¹⁰	s ⁻¹

Symbol	Variable	Calculated (CA)	Source	CODATA ₂₀₁₈ (CD) © COBE Data	±Accuracy	Δy (CA/CD-1)	Unit
cR _∞	cR _∞	3.289841962699988·10 ¹⁵	C	3.289841960250864·10 ¹⁵	1.9·10 ⁻¹²	+7.44450·10 ⁻¹⁰	Hz
H ₀	H0	2.223925234581364·10 ⁻¹⁸	C	2.223376656062923·10 ⁻¹⁸	1.1385·10 ⁻³	+2.46732·10 ⁻⁴	s ⁻¹
H ₀	HPC[Q0]	68.62410574852400	C	68.60717815146482←↑⊙	1.1385·10 ⁻³	+2.46732·10 ⁻⁴	kms ⁻¹ Mpc ⁻¹
q ₁	q1	1.527981474087040·10 ¹²	F	n.a.	n.a.	unusual	As
q ₀	q0	5.290817689717126·10 ⁻¹⁹	C	5.2908176897171 ·10 ⁻¹⁹	calculated	+4.44089·10 ⁻¹⁵	As
e	qe	1.602176634000007·10 ⁻¹⁹	C	1.602176634 ·10 ⁻¹⁹	exactly	+4.44089·10 ⁻¹⁵	As
U ₁	U1	8.698608435529670·10 ⁸⁷	F	n.a.	n.a.	unusual	V
U ₀	U0	1.042939697003725·10 ²⁷	C	1.042939697286845·10 ²⁷	calculated	-2.71463·10 ⁻¹⁰	V
W ₁	W1	1.360717888312544·10 ¹³¹	F	n.a.	n.a.	unusual	J
W ₀	W0	1.956081416291675·10 ⁹	C	1.956081416291641·10 ⁹	calculated	+1.73195·10 ⁻¹⁴	J
W _{k1}	Wk1	6.301953910302633·10 ¹²⁶	C	n.a. k→CMBR	n.a.	unusual	J
S ₁	S1	5.605711433987692·10 ⁴²⁶	F	n.a.	n.a.	unusual	Wm ⁻²
S ₀	S0	1.388921881877266·10 ¹²²	C	n.a.	n.a.	unusual	Wm ⁻²
S _{k1}	Sk1	2.596200130940090·10 ⁴²²	C	n.a. k→CMBR	n.a.	unusual	Wm ⁻²
S _{k0}	Sk0	1.251454657497949·10 ⁻⁵	C	1.25013 ·10 ⁻⁵	+1.0596·10 ⁻³	calculated [59]	Wm ⁻²
σ _e	σe	6.652458724888907·10 ⁻²⁹	C	6.6524587321600 ·10 ⁻²⁹	9.1·10 ⁻¹⁰	-1.09299·10 ⁻⁹	m ²
a _e	ae	1.159652181281556·10 ⁻³	C	1.1596521812818 ·10 ⁻³	1.5·10 ⁻¹⁰	-2.10054·10 ⁻¹³	1
g _e	ge	-2.00231930436256	C	-2.00231930436256	1.7·10 ⁻¹³	-2.22045·10 ⁻¹⁶	1
γ _e	γe	1.760859630228709·10 ¹¹	C	1.7608596302353 ·10 ¹¹	3.0·10 ⁻¹⁰	-3.74278·10 ⁻¹²	s ⁻¹ T ⁻¹
μ _e	μe	-9.28476469866128·10 ⁻²⁴	C	-9.284764704328 ·10 ⁻²⁴	3.0·10 ⁻¹⁰	-6.10325·10 ⁻¹⁰	JT ⁻¹
μ _B	μB	-9.27401007265130·10 ⁻²⁴	C	-9.274010078328 ·10 ⁻²⁴	3.0·10 ⁻¹⁰	-6.12109·10 ⁻¹⁰	JT ⁻¹
μ _N	μN	5.050783742986264·10 ⁻²⁷	C	5.0507837461150 ·10 ⁻²⁷	3.1·10 ⁻¹⁰	-6.19456·10 ⁻¹⁰	JT ⁻¹
Φ ₀	Φ0	2.067833847194937·10 ⁻¹⁵	C	2.067833848 ·10 ⁻¹⁵	exactly	-3.89327·10 ⁻¹⁰	Wb
G ₀	GQ0	7.748091734611053·10 ⁻⁵	C	7.748091729000002·10 ⁻⁵	exactly	+7.24185·10 ⁻¹⁰	S
K _J	KJ	4.835978487132911·10 ¹⁴	C	4.835978484 ·10 ¹⁴	exactly	+6.47834·10 ⁻¹⁰	HzV ⁻¹
R _K	RK	2.581280744348851·10 ⁴	C	2.581280745 ·10 ⁴	exactly	-2.52258·10 ⁻¹⁰	Ω
α	alpha	7.297352569776440·10 ⁻³	F	7.297352569311 ·10 ⁻³	1.5·10 ⁻¹⁰	+6.37821·10 ⁻¹¹	1
δ	delta	9.378551014802563·10 ⁻¹	F	9.378551009654370·10 ⁻¹	1.5·10 ⁻¹⁰	+5.48932·10 ⁻¹⁰	1
χ̄	xtiilde	2.821439372122070	F	2.821439372	mathematical	real number	1
σ ₁	σ1	9.773258655978905·10 ⁻¹⁹¹	F	n.a.	calculated	unusual	Wm ⁻² K ⁻⁴
σ	σ	5.670366673885496·10 ⁻⁸	C	5.670366673885496·10 ⁻⁸	exactly	exactly	Wm ⁻² K ⁻⁴

S Subspace value (const) M Magic value
 F Fixed value (invariable) C Calculated (calculated)

MachinePrecision → ±2.22045·10⁻¹⁶
 MOOP Matter of Opinion

Table 5:
 Universal natural constants
 Concerted International System of Units

11. References

- [1] **Gerd Pommerenke**
The Shape of the Universe, Augsburg 2021 (2005-2013, 2020-2021) *viXra:1310.0189*
6th reworked edition, please update elder editions
- [2] **Ottmar Marti**
Institut für Experimentelle Physik, Universität Ulm
Strahlungsgesetze
<http://wwwex.physik.uni-ulm.de/lehre/gk4-2005/node13.html>
(Last accessed: 29. July 2020, 15:08 UTC)
- [3] **Prof. Dr. sc. techn. Dr. techn. h.c. Eugen Philippow**, TH Ilmenau
Taschenbuch der Elektrotechnik, Band 2, Grundlagen der Informationstechnik
Verlag Technik Berlin. 1. Auflage 1977
ASIN: B008365UYE
- [4] **Seite „Grauer Körper“**
Wikipedia, Die freie Enzyklopädie. Bearbeitungsstand: 19. April 2018, 09:53 UTC.
https://de.wikipedia.org/w/index.php?title=Grauer_K%C3%B6rper&oldid=176666036
(Last accessed: 29. July 2020, 12:53 UTC)
- [5] **Seite „Wiensches Verschiebungsgesetz“**
Wikipedia, Die freie Enzyklopädie. Bearbeitungsstand: 12. Juni 2020, 11:03 UTC.
https://de.wikipedia.org/w/index.php?title=Wiensches_Verschiebungsgesetz&oldid=200891873
(Last accessed: 5. August 2020, 06:58 UTC)
- [6] **Dipl. Ing. Gerd Pommerenke**
The Electron and Weak Points of the Metric System, Augsburg 2022 *viXra:2201.0122*
DOI: 10.13140/RG.2.2.32859.64801/2
- [7] **Gerd Pommerenke**
The Metric Universe, 3rd edition, Augsburg 2023 *viXra:2209.0026 and RG*
DOI: 10.13140/RG.2.2.27826.48324/1
- [8] **Manfred Zollner**
www.gitec-forum.de
Negative Laufzeit – Gibt's die wirklich?, © 2017
https://cdn.website-editor.net/80f045601f964fd4933c7d1f5e98a4ad/files/uploaded/Z22_Gruppenlaufzeit.pdf
(Last accessed: 22. February 2022, 18:03 UTC maybe moved in the meantime, ask me for the file)
- [9] **H.-J. Treder† (Herausgeber)**, Gravitationstheorie und Theorie der Elementarteilchen,
Wiederabdruck ausgewählter Beiträge des Einstein-Symposiums 1965 in Berlin
Cornelius Lanczos†, Dublin, Irland,
»Tetraden-Formalismus und definite Raum-Zeit-Struktur«,
Akademieverlag, Berlin (O) 1979, S. 24 ff. (German)
- Alternative source German: *viXra:1906.0321* pp. 9-15
Alternative source English : *viXra:1310.0189* pp. 9-15
- MLA
Treder, H J. Gravitation theory and theory of elementary particles. Reprint of selected papers of the Einstein symposium held in Berlin, 1965. Gravitationstheorie und Theorie der Elementarteilchen. Wiederabdruck ausgewählter Beiträge des Einstein-Symposiums 1965 in Berlin. Germany: N. p., 1979. Web.
ISBN: none, Lizenznummer:202 • 100/559/78, Bestellnummer: 762 6051 (6506) • LSV 1115
- [10] **Seite „Wiensches Verschiebungsgesetz“**
Wikipedia, Die freie Enzyklopädie. Bearbeitungsstand: 16. Juni 2022, 11:41 UTC.
https://de.wikipedia.org/w/index.php?title=Wiensches_Verschiebungsgesetz&oldid=223744644
(Last accessed: 25. July 2022, 08:59 UTC)
- [11] **Gernot Neugebauer, Relativistische Thermodynamik**,
Akademieverlag, Berlin (O) 1980
ISBN: 978-3528068639
- [12] **Wikipedia contributors. “Cosmic microwave background”**
Wikipedia, The Free Encyclopedia. December 3, 2021, 18:12 UTC.
https://en.wikipedia.org/w/index.php?title=Cosmic_microwave_background&oldid=1058466831
(Last accessed: 16. December 2021, 17:30 UTC)
- [13] **Huntemann. N. and Lipphardt. B. and Tamm. Chr. and Gerginov. V. and Weyers. S. and Peik. E.**
Improved Limit on a Temporal Variation of mp/me from Comparisons of Yb+ and Cs Atomic Clocks
American Physical Society, 10.1103/PhysRevLett.113.210802. Nov. 2014
<https://link.aps.org/doi/10.1103/PhysRevLett.113.210802>
- [14] **Gerd Pommerenke**
Expansion, Topology and Entropy, Augsburg 2021 *viXra:2106.0063 and RG*
DOI: 10.13140/RG.2.2.29504.20482



Envelope Curve Approximation

Declarations

```
Off[InterpolatingFunction::dmval]
Off[FindMaximum::lstol]
Off[FindRoot::nlnum]
Off[General::spell]
Off[General::spell1]
Off[Greater::nord]
Off[NIntegrate::inumr]
Off[NIntegrate::precw]
Off[NIntegrate::ncvb]
```

Units

```
km = 1000;
Mpc = 3.08572*10^19 km;
minute = 60;
hour = 60 minute;
day = 24*hour;
year = 365.24219879*day;
Mo = 1.98840*10^30;
Ro = 6.96342*10^8;
ME = 5.9722*10^24;
RE = 6.371000785*10^6;
```

Basic Values

```
c=2.99792458*10^8; (*Speed of light*);
my0=4 Pi 10^-7; (*Permeability of vacuum*);
ka0=1.3697776631902217*10^93; (*Conductivity of vacuum*);
hb1=8.795625796565464*10^26; (*Planck constant slashed init*);
k=1.3806485279*10^-23; (*Boltzmann constant*);
me=9.109383701528*10^-31; (*Electron rest mass with Q0 Magic value 1*);
mp=1.6726219236951*10^-27; (*Proton rest mass Magic value 2*);
```

Auxilliary Values

```
mep=SetPrecision[me/mp,20]; (*Mass ratio e/p*);
ma=1822.8884862171988 me; (*Atomic mass unit*);
ϵ=ArcSin[0.3028221208819742993334500624769134447]-3Pi/4; (*RnB angle ϵ null(fix)*);
γ=Pi/4-ϵ; (*RnB angle γ nullvector*);
ζ=1/(36Pi^3)(3Sqrt[2])^(-1/3)/mep; (*re-correction factor*);
xtilde=3+N[ProductLog[-3E^-3]]; (*Wien displacement law constant (v)*);
alpha=Sin[Pi/4-ϵ]^2/(4Pi); (*Correction factor QED \[Alpha](Q0)*);
delta=4Pi/alpha*mep; (*Correction factor QED \[Delta](Q0)*);
(*Q0=(9Pi^2 Sqrt[2]delta me/my0/ka0/hb0SI)^(-3/4) (*Phase Q0=2ω0t during calibration*);*)
Q0=(9 Pi^2 Sqrt[2]delta me/my0/ka0/hb1)^(-3/7); (*Phase Q0=2ω0t after calibration*);
```

Composed expressions

```
Z0=my0 c; (*Field wave impedance of vacuum*);
ep0=1/(my0 c^2) (* Permittivity of vacuum*);
R∞=1/(72 Pi^3)/r1 Sqrt[2] alpha^2 /delta Q0^(-4/3); (*Rydberg constant*);
Om1=ka0/ep0; (*Cutoff frequency of subspace*);
Om0=Om1/Q0; (*Planck's frequency*);
OmR∞=2 Pi c R∞; (*Rydberg angular frequency*);
cR∞=c R∞; (*Rydberg frequency*);
H0=Om1/Q0^2; (*Hubble parameter local*);
H1=3/2*H0; (*Hubble parameter whole universe*);
r1=1/(ka0 Z0); (*Planck's length subspace*);
a0=9Pi^2 r1 Sqrt[2] delta/alpha Q0^(4/3); (*Bohr radius*);
lbarC=a0 alpha; (*Reduced Compton wavelength*);
```

```

ΛC=2 Pi ΛbarC; (*Compton wavelength electron*);
re= r1 (2/3)^(1/3)/ζ Q0^(4/3); (*Classic electron radius*);
r0= r1 Q0; (*Planck's length vac*);
R= r1 Q0^2; (*World radius*);
RR=R/Mpc/1000; (*World radius Gpc*);
t1=1/(2 Om1); (*Planck time subspace*);
t0=1/(2 Om0); (*Planck time vacuum*);
T=1/(2 H0); (*World time constant*);
TT=2T/year; (*The Age*);
hb0=hb1/Q0; (*Planck constant slashed*);
h0=2Pi*hb0; (*Planck constant unslashed*);
q1=Sqrt[hb1/Z0]; (*Universe charge*);
q0=Sqrt[hb1/Q0/Z0]; (*or qe/Sin[π/4-ε] Planck charge*);
qe=q0 Sin[Pi/4-ε]; (*Elementary charge e*);
M2=my0 ka0 hb1; (*Total mass with Q=1*);
M1=M2/Q0; (*Mach mass*);
m0=M2/Q0^2; (*Planck mass downwardly*);
(*m0=(9Pi^2Sqrt[2]*delta*me)^.75*(my0*ka0*hb0SI)^.25; (*Planck mass upwardly*);*)
mp=4Pi me/alpha/delta; (*Proton rest mass with Q0*);
(*me=Sqrt[hb1/Q0/Z0]*Sin[Pi/4-ε]; (*if using Q0 as Magic value*);*)
MH=M2/Q0^3; (*Hubble mass*);
G0=c^2*r0/m0; (*hb0*c/m0^2*); (*Gravity constant local*);
G1=G0/Q0^2; (*Gravity constant Mach*);
G2=G0/Q0^3; (*Gravity constant Init*);
U0=Sqrt[c^4/4/Pi/ep0/G0]; (*Planck voltage generic*);
U1=U0*Q0; (*Planck voltage Mach*);
W1=Sqrt[hb1 c^5/G2]; (*Energy with Q=1*);
W0=W1/Q0^2; (*Planck energy*);
S1=hb1 Om1^2/r1^2; (*Poynting vector metric with Q=1*);
S0=S1/Q0^5; (*Poynting vector metric actual*);
Sk1=4Pi^2*E^2/18^4/60*hb1*Om1^2/r1^2; (*Poyntingvec CMBR initial*);
Sk0=Sk1/Q0^4/Q0^3/E^2; (*Poyntingvec CMBR actual*);
wk1=Sk1/c; (*Energy density CMBR initial*);
wk0=Sk0/c; (*Energy density CMBR actual*);
Wk1=wk1*r1^3; (*Energy CMBR initial*);
μB=-9/2Pi^2 Sqrt[2 hb1/Z0]delta Sin[γ]/my0/ka0 Q0^(5/6); (*Bohr magneton*);
μN=-μB*mep; (*Nuclear magneton*);
μe=1.0011596521812818 μB (*Electron magnetic moment*);
Tk1=hb1 Om1/18/k; (*CMBR-temperature Q=1*);
Tk0=Tk1/Q0^(5/2); (*CMBR-temperature*);
Tp0=0.; Tp1=0.; (*Planck-temperature*);
φ0=Pi Sqrt[hb1 Z0/Q0 ]/Sin[Pi/4-ε]; (*Magnetic flux quantum Pi ħ/e*);
GQ0=1/Pi/Z0*Sin[Pi/4-ε]^2; (*Conductance quantum e^2/Pi ħ*);
KJ=2q0 Sin[Pi/4-ε]/h0; (*Josephson constant 2e/h*);
RK=.5 my0 c/alpha; (*von Klitzing constant μ0c/2α*);
σe=8Pi/3 re^2; (*Thomson cross section (8Pi/3)re^2*);
ae=SetPrecision[μe/μB,20]-1; (*Electron magnetic moment anomaly*);
ge=-2(1+ae); (*electron g-factor*);
ye=2 Q0 Abs[μe]/hb1; (*electron gyromagnetic ratio*);
σ1= SetPrecision[Pi^2/60 k^4/c^2/hb1^3, 16]; (*Stefan-Boltzmann constant initial*);
σ=σ1*Q0^3; (*Stefan-Boltzmann constant*);

```

Basic Functions

```

cMc=Function[-2 I/#/Sqrt[1-(HankelH1[2,#]/HankelH1[0,#])^2]];
Qr=Function[#1/Q0/2/#2];
PhiQ=Function[If[#>10^4,-Pi/4-3/4/#,
Arg[1/Sqrt[1-(HankelH1[2,#]/HankelH1[0,#])^2]]-Pi/2]]; (*Angle of c arg θ(Q)*);
PhiR=Function[PhiQ[Qr[#1,#2]]];
RhoQ=Function[If[#<10^4,N[2/#/Abs[Sqrt[1-
(HankelH1[2,#]/HankelH1[0,#])^2]]],1/Sqrt[#]]];
RhoR=Function[RhoQ[Qr[#1,#2]]];
AlphaQ=Function[Pi/4-PhiQ[#]]; (*Angle α*);
AlphaR=Function[N[Pi/4-PhiR[#1,#2]]];
BetaQ=Function[Sqrt[#1]*((#2)^2+#1^2*(1-(#2)^2)^(-.25)];
GammaPQ=Function[N[PhiQ[#]+ArcCos[RhoQ[#]*Sin[AlphaQ[#]]]+Pi/4]];
rq={{0,0}};
For[x=-8;i=0,x<4,++i,x+=.01;AppendTo[rq,{10^x,N[10^x*RhoQ[10^x]]}]];
RhoQ1=Interpolation[rq];
RhoQQ1=Function[If[#<10^3,RhoQ1[#],Sqrt[#]]]; (*Interpolation RhoQ*);

```

```

Rk=Function[If[#<10^5,3/2*Sqrt[#]*NIntegrate[RhoQQ1[x],{x,0,#}],6#]];
Rn=Function[Abs[3/2*Sqrt[#]*NIntegrate[RhoQQ1[x]*Exp[I*(PhiQ[x])],{x,0,#}]]];
RnB=Function[Arg[NIntegrate[RhoQQ1[x]*Exp[I*(PhiQ[x])],{x,0,#}]]];
alphaF=Function[Sin[Pi/2+ε-(*RNBP*)RnB[#]]^2/(4Pi)]; (*RNBP defined behind End of...*);
deltaF=Function[4Pi/alphaF[#]*mep]; (*Correction factor QED δ(Q)*);

```

End of Metric System Definition

Functions Used for Calculations in Articles

```

GV=Function[Graphics[Line[{{#1,#2},{#1,#3}}]]]; (*Graphics help function*);
GH=Function[Graphics[Line[{{#2,#1},{#3,#1}}]]]; (*Graphics help function*);
Xline=Function[10^33*(#1-#2)]; (*Value_x vertical line*);
ExpP=Function[If[#<0,1/Exp[-#],Exp[#]]]; (*To avoid calculation errors*);
FG = Function[.5/(1 + I*#)*(1 + 1/(1 + I*#))];
Xline = Function[10^33*(#1 - #2*(Wert_x*))];
Pom = Function[Print[StringJoin["x = ",
  ToString[10^Chop[First[xx /. Rest[%]], 10^-7]], " Om1",
  " (" , ToString[.5*10^Chop[First[xx /. Rest[#]], 10^-7]],
  " OmU)"]];];
Pol = Function[Print["y = " <> ToString[First[#]] <> " dB (" <>
  If[First[#] - zzz > 0, "+", ""] <> ToString[First[#] - zzz] <>
  " dB)"];];

BRQP = Function[Rk[#] Sqrt[(Sin [AlphaQ[#]]/Sin[GammaPQ[#]])^4 - 1]];
BGN = Sqrt[2]*BRQP[.5]/3;
gdc = Function[10^(Log10[E]*(-1) (1*#)^2/(1 + 1*#^2)^2)]; (*Group Delay Correction*);
cc = xtilde^2;
b = xtilde;
s1 = 8*(#1/(2*((#1/2)^2 + 1)))^2 & ;
s2 = (b*(#1/2))^3/(ExpP [b*(#1/2)] - 1) & ;
brq = {{0, 0}};
For[x = -8; i = 0, x < 50, (++i), x += .05;
  AppendTo[
    brq, {10^x, N [BRQP[10^x]/BGN/(2.5070314770581117*10^x) ]}]]];
BRQ0 = Interpolation [brq];
BRQ1 = Function[If[# < 8*10^4, BRQ0[#], Sqrt[#]]];
Psi1 = NIntegrate[(1/2)*Log[1 + (#1/(cc*Sqrt[Q]))^2] -
  ((#1/(cc*Sqrt[Q]))^2)/(1 + (#1/(cc*Sqrt[Q]))^2) -
  Log[Cos[-ArcTan[#1/(cc*Sqrt[Q])] +
  #1/(cc*Sqrt[Q])/(1 + (#1/(cc*Sqrt[Q]))^2)]]],
  {Q, 0.5, 3000}] & ; (*Approximation*);
Psi2 = NIntegrate[(1/2)*Log[1 + (#1/(cc*BRQ1[Q]))^2] -
  ((#1/(cc*BRQ1[Q]))^2)/(1 + (#1/(cc*BRQ1[Q]))^2) -
  Log[Cos[-ArcTan[#1/(cc*BRQ1[Q])] +
  #1/(cc*BRQ1[Q])/(1 + (#1/(cc*BRQ1[Q]))^2)]]],
  {Q, 0.5, 3000}] & ; (*Exact ξ*);
HPC = Function[Om1/#^2/km*Mpc]; (*H0=f(Q0) [km*s-1*Mpc-1]*);
ff = 4/3/18^3/9/15/Sqrt[2]/delta ma/me;
fff = 4/3/18^3/9/15/Sqrt[2] ma/me;
gg = N[1.48 Pi^2/60/18^3];
ngN = Function[gg/r1^3/#^4.5];
nmN = Function[3.7 (gg/r1^3/#^4.5)/(fff*#^(1/6))];
Gmin = qqg /.
  FindRoot[
    N[ngN[qqg]]*N[r1^3 (qqg)^4.5 BRQ1[qqg]^3] - 32 == 0, {qqg, 1, 100}];

```

Helpful Interpolations

Not really needed. Evaluate only once the lines below the upper lines, then store data in e.g. rs={data} and close the cells. Evaluation can take a while. Don't delete but always evaluate them. Disable evaluation for the lines below the upper line until Interpolation line then. Save notebook.

```

rs={"Insert output from below"};
rs={};
For[x=(-3); i=0,x<3,(++i),x+=.025;
  AppendTo[rs,{10^x,NIntegrate[RhoQQ1[z],{z,0,10^x}]/Abs[NIntegrate[RhoQQ1[z]*
  Exp[I/2*ArgThetaQ[z]],{z,0,10^x}]]}]]];

```

```
rs
RS=Interpolation[rs]; (*Relation rk/rn*);
RS1=Function[1/RS[#]];
```

```
rnb={"Insert output from below"};
rnb={};
For[d=-6.01; i=0,d<6.01,(++i),d+=.05; AppendTo[rnb,{d,RnB[10^d]/Pi}]]
rnb

RNB1=Interpolation[rnb]; (*RnB angle  $\epsilon$  nullvector from Q*);
RNB=Function[If[#<10^-8,Null,If[#<10^6,RNB1[Log10[#]],-.25]]];
RNBPF=Function[If[#<10^-8,Null,If[#<10^6,Pi RNB1[Log10[#]],-Pi/4]]];
alphaF=Function[Sin[Pi/2+ $\epsilon$ -RNBPF[#]]^2/(4 Pi)]; (* Faster redefinition *);
```

```
qq1={"Insert output from below"};
qq1={};
For[xy=(-17); i=0,xy<5,(++i),xy+=.05; AppendTo[qq1,{10^xy,N[Sin[(Pi/2-
RnB[10^xy]+ $\epsilon$ )]}]]]
qq1

QQ0=Interpolation[qq1]; (*Relation qe/q0*);
QQ=Function[If[#<10^5,QQ0[#],0.3028223504900885]];
QQ1=Function[If[#<10^5,1/QQ0[#],3.3022661582990733]];
```

```
inb={"Insert output from below"};
inb={};
For[d=-6.01; i=0,d<6.01,(++i),d+=.05; AppendTo[inb,{RnB[10^d]/Pi,d}]]
inb

INB1=Interpolation[inb]; (*InvRnB Q from angle  $\epsilon$  nullvector*);
INB=Function[Which[-1<#<0,INB1[#],#==0,3/2Pi Q0^.25,#>0,Null]];
INBPF=Function[Which[-Pi<#<0,INB1[#/Pi],#==0,3/2 Q0^.25,#>0,Null]];
```

Approximation

```
(*b = xtilde; Figure3 *)
Plot[{
Log10[(b*.5*10^y)^3/(Expp[b*.5*10^y]-1)],
Log10[ 8*(.5*10^y)/((.5*10^y)^2+1)^2],
Xline[y,Log10[2]]},{y,-5,3},PlotRange->{-10.1,.45}]
```

Expansion

```
Plot[{(*Log10[BRQP[10^qqq]/BGN/(2.5070314770581117*10^qqq)], Figure4a *)
Log10[BRQ1[10^qqq]], Log10[Sqrt[10^qqq]]}, {qqq,-1,10}]
Plot[{(*BRQP[qqq]/BGN/(2.5070314770581117*qqq), Figure4b *)
BRQ1[qqq], Sqrt[qqq]}, {qqq,0,10}, PlotRange->{-0.3,9.6}]
```

Integral

```
cc=8; (*Factor 8 approx  $\xi$  Figure5 *)
Plot[{Psi1[y],Psi2[y]}, {y,0.001,10},
PlotStyle->RGBColor[0.91,0.15,0.25],
PlotLabel->None,LabelStyle->{FontFamily->"Chicago",10,Black}]

cc=8; (*Factor 8 approx  $\xi$  Figure6 *)
b3=Plot[{10Log10[Expp[Psi1[10^y]]],10 Log10[Expp[Psi2[10^y]]]}, {y,-3,2},
PlotRange->{-88,2},LabelStyle->{FontFamily->"Chicago",12,Black}];

b4=Plot[{10 Log10[Abs[FG[10^y]]]}, {y,-3,2},PlotRange->{-88,2},PlotLabel->None,
PlotStyle->RGBColor[0,0,0],LabelStyle->{FontFamily->
>"Chicago",10,Black,PlotRangeClipping->True}];

Show[b3,b4]
```


Approximation 1

```
cc=8; (* Factor 8 approximated BGN exact Figure7 *)
Plot[{10 Log10[s2[10^y]],10 (Log10[s1[10^y]*Exp[Psi1[10^y]]]},Xline[y,Log10[2]]},
{y,-3,3},PlotRange->{-51,10.5},ImageSize->Full,LabelStyle->{FontFamily->
>"Chicago",10,Black}] (* Exact exact exact error max +1.3dB *)

cc=7.519884824; (* Sqrt[n] exact Figure8 *)
Plot[{10 Log10[s2[10^y]],10
(Log10[s1[10^y]]+Log10[E]*Psi2[10^y]),Xline[y,Log10[2]]},{y,-3,3},
PlotRange->{-51,4.5},ImageSize->Full,LabelStyle->{FontFamily->"Chicago",10,
Black}] (* Exact exact exact error max +1.3dB *)
```

Extrema 1

```
u=FindMaximum[10 Log10[s2[10^xx]],{xx, 0}];
(* Planck's curve *)
Print[StringJoin["x = ",ToString[(10^First[xx/.Rest[u]])," Om1      (1.000000
OmU)"]]
Print[StringJoin["y = ",ToString[z = First[u]]," dB      (±0.000000 dB)"]]

FindMaximum[10 (Log10[s1[10^xx]*Exp[Psi1[10^xx]])-10Log10[s2[10^xx]],{xx,0}];
(* Maximum deviation 1 Psi1 *)
Pom[%]
Pol[%%]

FindMinimum[10 (Log10[s1[10^xx]*Exp[Psi1[10^xx]]/s2[10^xx]),{xx,2}];
(* Maximum deviation 2 Psi1 *)
Pom[%]
Pol[%%]

FindMaximum[10 (Log10[s1[10^xx]*Exp[Psi2[10^xx]])-10Log10[s2[10^xx]],{xx,0}];
(* Maximum deviation 1 Psi2 *)
Pom[%]
Pol[%%]

FindMaximum[10 (Log10[s1[10^xx]*Exp[Psi2[10^xx]])-10Log10[s2[10^xx]],{xx,1}];
(* Maximum deviation 2 Psi2 *)
Pom[%]
Pol[%%]

FindMaximum[10 (Log10[s1[10^xx]]+Log10[E]*Psi1[10^xx]),{xx,0}];
(* Deviation between maxima Psi1*)
Pom[%]
Pol[%%]

FindMaximum[10 (Log10[s1[10^xx]]+Log10[E]*Psi2[10^xx]),{xx,0}];
(* Deviation between maxima Psi2 *)
Pom[%]
Pol[%%]
```

Deviation 1

```
cc=8; (*Factor 8 approx Figure9 *)
b71=Plot[{10 Log10[s1[10^y]*Exp[Psi1[10^y]]/s2[10^y]],Xline[y,Log10[2]]},
{y,-3,2},PlotRange->{-3.02,1.42},ImageSize->Full,LabelStyle->{FontFamily->
"Chicago",10,Black}];

cc=7.519884824; (* Sqrt[n] exact Figure8 *)
b72=Plot[{10 Log10[s1[10^y]*Exp[Psi2[10^y]]/s2[10^y]],{y,-3,2},ImageSize->Full,
LabelStyle->{FontFamily->"Chicago",10,Black}];
b73=Plot[{-10 Log10[gdc[10^x]],{x,-3,2.2},PlotRange->{-3.02,1.42},
PlotStyle->RGBColor[0.06,0.52,0.]];

Show[b71,b72,b73,ImageSize->Full,LabelStyle->{FontFamily->"Chicago",12,Black}]
```

Approximation 2

```
cc=8; (* Factor 8 approximated BGN exact Figure10 *)
Plot[{10 Log10[s2[10^y]],10 (Log10[s1[10^y]*Exp[Psi1[10^y]]]+
```

```
10Log10[gdc[10^y]],Xline[y,Log10[2]]},{y,-3,3},PlotRange->{-51,4.5},
ImageSize->Full,LabelStyle->{FontFamily->"Chicago",10,Black}}
(* Exact exact exact error max +1.3dB *)
```

```
cc=7.519884824; (* Sqrt[n] exact { Figure11 *)
Plot[{10 Log10[s2[10^y]],10 (Log10[s1[10^y]]+Log10[E]*Psi2[10^y])+
10Log10[gdc[10^y]],Xline[y,Log10[2]]},{y,-3,3},PlotRange->{-51,4.5},
ImageSize->Full,LabelStyle->{FontFamily->"Chicago",10,Black}}
(* Exact exact exact deviation max +1dB *)
```

Extrema 2

```
v=FindMaximum[10 Log10[s2[10^xx]],{xx, 0}];
(* Planck's curve *)
Print[StringJoin["x = ",ToString[(10^First[xx/.Rest[v]])], " Om1      (1.000000
OmU) "]]
Print[StringJoin["y = ",ToString[zzz = First[v]], " dB      (±0.000000 dB)"]]

FindMaximum[10 Log10[(s1[10^xx]*Expp[Psi1[10^xx]]*gdc[10^xx])/s2[10^xx]],{xx,0}];
(* Maximum deviation 1 Psi1 *)
Pom[%]
Pol[%%]

FindMaximum[10 Log10[(s1[10^xx]*Expp[Psi2[10^xx]]*gdc[10^xx])/s2[10^xx]],{xx,0}];
(* Maximum deviation 1 Psi2 *)
Pom[%]
Pol[%%]

FindMinimum[10 Log10[(s1[10^xx]*Expp[Psi2[10^xx]]*gdc[10^xx])/s2[10^xx]],{xx,.5}];
(* Maximum deviation 2 Psi2 *)
Pom[%]
Pol[%%]

FindMaximum[10 Log10[(s1[10^xx]*Expp[Psi2[10^xx]]*gdc[10^xx])/s2[10^xx]],{xx,1}];
(* Maximum deviation 3 Psi2 *)
Pom[%]
Pol[%%]

FindMaximum[10 Log10[s1[10^xx]*Expp[Psi1[10^xx]]*gdc[10^xx]],{xx,0}];
(* Deviation between maxima Psi1 *)
Pom[%]
Pol[%%]

FindMaximum[10 Log10[s1[10^xx]*Expp[Psi2[10^xx]]*gdc[10^xx]],{xx,0}];
(* Deviation between maxima Psi2 *)
Pom[%]
Pol[%%]

Plot[({ Figure12 *)
  10 Log10[s1[10^y]],
  10 Log10[s2[10^y]],
  10 (Log10[s1[10^y]]+Log10[E]*Psi2[10^y]),
  10 (Log10[s1[10^y]]+Log10[E]*Psi2[10^y]+Log10[gdc[10^y]]),
  Xline[y,Log10[2]]
},{y,-0.8,1.4},PlotRange->{-11,4.5},PlotLabel->None,ImageSize->Full,LabelStyle-
>{FontFamily->"Chicago",10,Black}}
```

Deviation 2

```
cc=7.519884824; (* Sqrt[n] exact { Figure13 *)
b11=
  Plot[{10 Log10[s1[10^y]*Expp[Psi1[10^y]]/s2[10^y]]+10Log10[gdc[10^y]],
  10 Log10[s1[10^y]*Expp[Psi2[10^y]]/s2[10^y]]+10Log10[gdc[10^y]]},{y,
-3,2},ImageSize->Full,LabelStyle->{FontFamily->"Chicago",10,Black}];
Show[b11,b71,b72,b4,PlotRange->{-3.02,1.42}]
```

Nulls

```
n1=y/.FindRoot[10 (Log10[s1[10^y]]+Log10[E]*Psi2[10^y])+
10Log10[gdc[10^y]]-10Log10[s2[10^y]]==0,{y,0}]
```

```

n2=y/.FindRoot[10 (Log10[s1[10^y]]+Log10[E]*Psi2[10^y])+
  10Log10[gdc[10^y]]-10Log10[s2[10^y]]==0,{y,.75}]

n3=y/.FindRoot[10 (Log10[s1[10^y]]+Log10[E]*Psi2[10^y])+
  10Log10[gdc[10^y]]-10Log10[s2[10^y]]==0,{y,1.1}]

N[10^n1] (* Level at 1st null *)
ToString[10 Log10[s2[%]]]<>" dB"

N[10^n2] (* Level at 2nd null *)
ToString[10 Log10[s2[%]]]<>" dB"

N[10^n3] (* Level at 3rd null *)
ToString[10 Log10[s2[%]]]<>" dB"

N[10^1.4142] (* Level after 3rd null *)
ToString[10 Log10[s2[%]]]<>" dB"

```

Correlation

```

FindRoot[10 Log10[s2[10^yy]]+50==0,{yy,1.15,1.18}]
cc=8; (* Factor 8 approximated BGN exact Figure7 *)
cc=7.519884824; (* Sqrt[n] exact Figure8 *)
F2={};
For[y=-3;
  i=0,y<1.16415,++i,y+=.001;
  AppendTo[F2,N[10 Log10[s2[10^y]]]]];
cc=8; (* Factor 8 approximated BGN exact Figure7 *)
F5={};
For[y=-3;
  i=0,y<1.16415,++i,y+=.001;
  AppendTo[F5,N[10 (Log10[s1[10^y]]*Expp[Psi1[10^y]])]]];
cc=7.519884824; (* Sqrt[n] exact Figure8 *)
F6={};
For[y=-3;
  i=0,y<1.16415,++i,y+=.001;
  AppendTo[F6,N[10 (Log10[s1[10^y]]+Log10[E]*Psi2[10^y]])]]];
cc=8; (* Factor 8 approximated BGN exact Figure10 *)
F8={};
For[y=-3;
  i=0,y<1.16415,++i,y+=.001;
  AppendTo[F8,
  N[10 (Log10[s1[10^y]]*Expp[Psi1[10^y]])+10Log10[gdc[10^y]]]]];
cc=7.519884824; (* Sqrt[n] exact Figure11 *)
F9={};
For[y=-3;
  i=0,y<1.16415,++i,y+=.001;
  AppendTo[F9,N[10 (Log10[s1[10^y]]+Log10[E]*Psi2[10^y])+10Log10[gdc[10^y]]]]];
{Correlation[F5,F2],Correlation[F6,F2],Correlation[F8,F2],Correlation[F9,F2]}

```

Displacement line

```

b = xtilde;
b14=Plot[(* Figure14 *)
Log10[s2[10^y]], Log10[s1[10^y]],Xline[y,Log10[2]],
  2*y + Log10[2], 2*y - Log10[xtilde]], {y, -3.05, 3.05},
  PlotRange -> {0.55, -5.05}, ImageSize -> Full,
  LabelStyle -> {FontFamily -> "Chicago", 10, Black}]

```

Temperature CMBR

```

krz0 = qqg/.FindRoot[N[3.7ngN[qqg]]/
  N[fff*N[qqg]^(-4/3)*BRQ1[qqg]^3/deltaF[qqg]]*
N[r1 (qqg)^1.5 BRQ1[qqg]^3-32==0,{qqg,1,1.1}];
krz1 = qqg / .
  FindRoot[Log10[3.7 ngN[10^qqg]] - Log10[fff*N[10^qqg]^(-4/3)*
  BRQ1[10^qqg]^3/deltaF[10^qqg]] - Log10[ngN[10^qqg]] == 0, {qqg, 10, 20}];
krz2 = Log10[ngN[10^krz1]];

```

```

krz3 = Log10[nmN[10^krz1]] + 6 Log10[Sqrt[r1] N[10^krz1]];
krz4 = Log10[nmN[Q0]] + 6 Log10[Sqrt[r1] N[Q0]];
krz5 = Log10[ngN[Q0]] + 6 Log10[Sqrt[r1] N[Q0]];
xmin=Log10[krz0];
ymin=N[Log10[32]];

b15 = Plot[(* Figure15 *) {hb1 Om1/18/k/(2 T (1 + y) ka0/ep0)^1.25},
  {y, -0.52, 2}, PlotRange -> {0.4, 7.18}, AxesOrigin -> {0, 0.6903},
  ImageSize -> Full, PlotStyle -> Thickness[0.0038],
  LabelStyle -> {FontFamily -> "Chicago", 10, Black}]
b16 = Plot[(* Figure16 *) {Log10[hb1 Om1/18/k/(2*10^y ka0/ep0)^1.25]},
  {y, -107.5, 30}, PlotStyle -> {Thickness[0.004],
  RGBColor[0.5, 0.68, 0.37]}, PlotRange -> {-10, 168},
  ImageSize -> Full, AxesOrigin -> {0, 03},
  LabelStyle -> {FontFamily -> "Chicago", 10, Black}};
Show[b16,
  GH[Log10[1.41678] + 32, -107.5, 30],
  GV[Log10[9.53138*10^-9], -10, 168],
  GV[Log10[T], -10, 168],
  GV[Log10[t1/4], -10, 168]]

```

Exact world radius

```

b17a=Plot[(* Figure17 *)
  qq^1.5 BRQ1[qqq]],{qqq, 0, 3},
  LabelStyle->{FontFamily->"Chicago",13,Black},ImageSize->Full,
  PlotStyle->{RGBColor[0.27,0.39,0.54],Thickness[0.0035]}};
b17b=Plot[(* Figure17 *)
  qq^2},{qqq, 0, 3},
  LabelStyle->{FontFamily->"Chicago",13,Black},ImageSize->Full,
  PlotStyle->{RGBColor[1,0,.4],Thickness[0.0035]}};
Show[b17a,b17b,GV[0.5,-2,19]]

b18a=Plot[(* Figure18 *)
  Log10[(10^qqq)^1.5 BRQ1[10^qqq]],{qqq,-1,3},
  LabelStyle->{FontFamily->"Chicago",14,Black},ImageSize->Full,PlotRange->{-
  4.2,6.6},
  PlotStyle->{RGBColor[0.27,0.39,0.54],Thickness[0.0035]}};
b18b=Plot[(* Figure18 *)
  Log10[N[10^qqq]^2]],{qqq,-1,3},
  LabelStyle->{FontFamily->"Chicago",14,Black},ImageSize->Full,PlotRange->{-
  4.2,6.6},
  PlotStyle->{RGBColor[1,0,.4],Thickness[0.0035]}};
Show[b18a,b18b,GV[Log10[.5],-4.2,6.6]]

```

Maximum possible number of Line elements

```

b19a=Plot[(* Figure19 *)
  (qqq^0.5 BRQ1[qqq])^3}, {qqq, 0, 1.3}, PlotRange->{0,2.04},
  PlotStyle->{RGBColor[0.77,0.27,0.5],Thickness[0.0036]}};
b19b=Plot[(* Figure19 *)
  (qqq^-1 N[qqq]^2)^3}, {qqq, 0, 1.3}, PlotRange->{0,2.04},
  PlotStyle->{RGBColor[0.45,0.58,0.27],Thickness[0.0036]}};
Show[b19a,b19b,GV[N[.5],-6,18],GV[N[1],-6,18],
  GH[N[1],-6,18],GH[N[1.71454],-6,18],
  LabelStyle->{FontFamily->"Chicago",14,Black},ImageSize->Full]]

```

alphaF(Q,T) and deltaF(Q,T) immediately after BB

```

b20a=Plot[(* Figure20 *) {deltaF[(10^(t10)/t1)^.5]},
  {t10, (Log10[t1]-16), (Log10[t1]+16)}, ImageSize->Full,
  PlotLabel->None, LabelStyle->{FontFamily->"Chicago", 12, Black},
  AxesOrigin->{(Log10[t1]-15), 1}, PlotRange->{0, 1.03},
  PlotStyle->{RGBColor[0.51, 0.25, 0.5], Thickness[0.0035]}};
b20b=Plot[1/alphaF[10^t10]], {t10, -8, 8}, ImageSize->Full,
  PlotLabel->None, LabelStyle->{FontFamily->"Chicago", 12, Black},
  AxesOrigin->{8, 0}, PlotRange->{0, 150.4},
  PlotStyle->{RGBColor[0.51, 0.25, 0.5], Thickness[0.0035]}};
b20c=Show[b20b, GV[-0.18257004098843227, -8, 145], GV[0, -8, 145],

```

```

GH[12.566378870075917,-8,8],GH[137.0357912660098,-8,8],
GH[59.15105929915021,-8,8]];
Overlay[{b20a,b20c}]

b21a=Plot[(* Figure21 *) Log10[fff*N[10^qqq]^(-4/3)*BRQ1[10^qqq]^3/deltaF[10^qqq]],
{qqq,-.4,Log10[100Q0]},PlotStyle->{RGBColor[0.27,0.4,0.51],Thickness[0.0035]},
LabelStyle->{FontFamily->"Chicago",12,Black},ImageSize->Full];
b21b=Plot[(* Figure21 *)
Log10[ff*N[10^qqq]^(1/6)],{qqq,-.4,Log10[100Q0]},
PlotStyle->{RGBColor[1,0.21,0.38],Thickness[0.0035]},
LabelStyle->{FontFamily->"Chicago",12,Black},ImageSize->Full];
Show[b21a,b21b,GV[Log10[Q0],-8,80],GV[xmin,-5,10],
GH[Log10[ff Q0^(1/6)],-3,70],GH[Log10[ff (2/3)^(1/6)],-3,70]]
b22a=Plot[(* Figure22 *) Log10[fff*N[10^qqq]^(-
4/3)*BRQ1[10^qqq]^3/deltaF[10^qqq]],
{qqq,-1,5.05},PlotRange->{-4.05,1.85},PlotStyle->{RGBColor[0.27,0.39,0.54],
Thickness[0.0038]}];
b22b=Plot[(* Figure22 *) Log10[ff*N[10^qqq]^(1/6)],{qqq,-1,5.05},
PlotRange->{-4.05,1.85},PlotStyle->{RGBColor[1,0.21,0.38],Thickness[0.0038]}];
Show[b22a,b22b,GV[Log10[1/2],-5,2],GV[Log10[2/3],-5,2],GV[xmin,-5,2],
GH[Log10[fff*N[2/3]^(-4/3)*BRQ1[2/3]^3/deltaF[2/3]],-3,70],
GH[Log10[ff (1)^(1/6)],-3,70],GV[Log10[8238],-5,2],
LabelStyle->{FontFamily->"Chicago",12,Black},ImageSize->Full]

```

Photon - Nucleon - ratio/ m^3

```

b23a=Plot[(* Figure23 *)
Log10[3.7ngN[10^qqq]]-Log10[fff*N[10^qqq]^(-4/3)*
BRQ1[10^qqq]^3/deltaF[10^qqq]],{qqq,-1,Log10[100Q0]},
PlotStyle->{RGBColor[0.23,0.74,0.63],Thickness[0.0045]}];
b23b=Plot[(* Figure23 *)
Log10[ngN[10^qqq]],{qqq,-1,Log10[100Q0]},
PlotStyle->{RGBColor[0.91,0.43,0.5],Thickness[0.0045]}];
Show[b23a,b23b,GV[Log10[Q0],-30,350],GV[krz1,-30,350],GV[xmin,-30,350],
GH[Log10[ngN[Q0]],-3,70],GH[krz2,-30,350],AxesOrigin->{0,0},
LabelStyle->{FontFamily->"Chicago",12,Black},ImageSize->Full]

```

Real number of CMBR-photons and nucleons

```

krz1 "Equality x"
krz3 "Equality 10^x"
krz4 " Fermions nowadays"
krz5 "Bosons nowadays"
b24=Plot[(* Figure24 *)
Log10[ngN[10^qqq]]+3Log10[r1 (10^qqq)^1.5 BRQ1[10^qqq]],
Log10[ngN[10^qqq]]+6Log10[Sqrt[r1] N[10^qqq]],
Log10[3.7ngN[10^qqq]]-
Log10[fff*N[10^qqq]^(-4/3)*BRQ1[10^qqq]^3/deltaF[10^qqq]]+3*
Log10[r1 (10^qqq)^1.5 BRQ1[10^qqq]],
Log10[nmN[10^qqq]]+6Log10[Sqrt[r1] N[10^qqq]],{qqq,-.35,Log10[1000Q0]}];
Show[b24,GV[N[krz1],-20,100],GV[Log10[Q0],-20,100],GV[xmin,-20,100],
GV[3.91,-20,100],GH[ymin,-.5,70],
GH[krz3,-.5,70],GH[krz4,-.5,70],GH[krz5,-.5,70],
LabelStyle->{FontFamily->"Chicago",12,Black},ImageSize->Full]

```

Incoherent matter density

```

b25a=Plot[(* Figure25 *)
Log10[M2/(10^qqq)]-3 Log10[r1 (10^qqq)^1.5 BRQ1[10^qqq]]-3},
{qqq,-1,Log10[100 Q0]},PlotRange->{-45,435},
PlotStyle->{RGBColor[0.5,0.31,0.62],Thickness[0.0045]}];
b25b=Plot[(* Figure25 *)
Log10[M2/r1^3/(10^qqq)^7]-3},{qqq,-1,Log10[100 Q0]},PlotRange->{-45,435},
PlotStyle->{RGBColor[0.5,0.68,0.37],Thickness[0.0045]}];
Show[b25b,b25a,
GV[Log10[Q0],-45,440],GV[Log10[10^krz1],-45,440],
GH[Log10[7.00663*10^397],-3,70],GH[Log10[7.30066*10^263]-3,-3,70],
GH[Log10[7.41027*10^-26]-3,-3,70],LabelStyle->{FontFamily->"Chicago",12,
Black},ImageSize->Full,AxesOrigin->{0,0}]

```

Spatial dependence of incoherent matter density

```

q11=Function[Q0(1-(2#)^(2/3))];
b26=Plot[(* Figure26 *)
  Log10[N[M2/q11[qqq]]/N[r1 q11[qqq]^1.5 BRQ1[q11[qqq]]^3/10^3],
  Log10[N[M2/r1^3/q11[qqq]^7]/10^3]},{qqq,0,0.5},
  PlotRange->{-29.5,11},PlotStyle->RGBColor[0.333333, 0, 1]];
Show[b26,GV[0.5,-29.5,11],LabelStyle->{FontFamily->"Chicago",12,Black},
  ImageSize->Full,AxesOrigin->{0,Log10[M1/R^3]-3}]
M1/R^3/10^3

```